Copper excess promotes propagation and induces proteomic change in root cultures of *Hyoscyamus albus* L.

Ari Sako[a] · Jebunnahar Kandakar[b] · Noriko Tamari[b] · Ataru Higa[b] · Kenichi Yamaguchi[a, c] ·Yoshie Kitamura[a, b *]

[a] Graduate School of Fisheries and Environmental Sciences, Nagasaki University, Nagasaki 852-8521, Japan

[b] Graduate School of Science and Technology, Nagasaki University, Nagasaki 852-8521, Japan

[c] Division of Biochemistry, Faculty of Fisheries, Nagasaki University, Nagasaki 852-8521, Japan

[*]Corresponding author:

Yoshie Kitamura

Graduate School of Fisheries and Environmental Sciences, Nagasaki University, Nagasaki 852-8521, Japan.

Tel/Fax: +81-95-819-2759

E-mail: k-yoshie@nagasaki-u.ac.jp

Abstract

Hyoscyamus albus L. seedlings respond positively to copper (Cu) excess. In the present study, to understand how roots cope with Cu excess, propagation and proteome composition in the presence of Cu were examined using a root culture system. When *H. albus* roots were cultured in a medium without Cu, root growth deteriorated. However, in the presence of Cu, root growth increased in a concentration-dependent manner, and vigorous lateral root development was observed at 200 μM Cu. Cu accumulation in the roots increased with the Cu supply. Subcellular fractionation revealed that the highest amount of Cu was present in the cell wall-containing fraction, followed by the soluble fraction. However, the highest specific incorporation of Cu, in terms of fresh weight, was in the mitochondria-rich fraction. High Cu levels enhanced respiration activity. Comparative proteomic analysis revealed that proteins involved in carbohydrate metabolism, *de novo* protein synthesis, cell division, and ATP synthesis increased in abundance, whereas the proteasome decreased. These results indicate that Cu promotes propagation of *H. albus* roots through the activation of the energy supply and anabolism. Newly propagated root tissues and newly generated proteins that bind to Cu may provide space and reservoirs for deposition of additional Cu.

Keywords: copper; heavy metal; *Hyoscyamus albus*; proteomics; root culture; root respiration.

1. Introduction

Hyoscyamus spp. (Solanaceae) are well-known medicinal plants that produce tropane alkaloids, such as atropine (*dl*-hyoscyamine) and scopolamine, which are commercially important anticholinergic and sedative drugs (Evans, 2009). In a previous study, we determined that *Hyoscyamus albus* L. roots can survive iron (Fe) deficiency and that, under Fe-deficient conditions, they secrete riboflavin into the rhizosphere (Higa et al., 2010; 2012). To determine whether this phenomenon was specific to Fe deficiency, we examined the effect on root growth of deficiency in other essential metals, including manganese, zinc (Zn), molybdenum, and copper (Cu). We observed that the elimination of Cu seriously impaired growth, suggesting that *H. albus* roots are sensitive to Cu deficiency. A further study revealed that *H. albus* seedlings are tolerant to excess Cu (Tamari et al., 2014).

Cu is an essential heavy metal for both plants and humans. In plants, Cu is involved in a wide range of redox reactions that are essential for photosynthesis, respiration, ethylene perception, reactive oxygen metabolism, and cell-wall remodelling *via* Cu-containing proteins such as plastocyanin, Cu/Zn superoxide dismutase, and cytochrome *c* oxidase (Burkhead et al., 2009). The Cu content of nonpolluted soils worldwide ranges from 1 to 140 $mg.kg^{-1}$ dry weight, and Cu usually occurs in the form of poorly mobile compounds incorporated into carbonates, sulphates, organic matter, and clays (Terelak and Motowicka-Terelak, 2000).

However, Cu in its free form is very reactive in the presence of both thiols and oxygen and can promote oxidative stress (Ravet and Pilon, 2013; Sáez et al., 2015); therefore Cu excess is toxic to both animals and plants. Furthermore, the widespread industrial and agricultural uses of Cu cause serious Cu pollution, resulting in an increase in Cu mobility and bioavailability (Martins et al., 2012; Zou et al., 2015). A concentration of 3 μM or higher is considered a high level of Cu (Bernal et al., 2006). Some plants, denoted as Cu-excluders, survive by limiting Cu uptake and accumulation, whereas others that actively uptake Cu, rapidly transport it, and then efficiently accumulate Cu in shoots are defined as accumulators/hyperaccumulators (Masarovičová et al., 2010; Visioli and Marmiroli, 2013). In our previous study, we reported that *H. albus* seedlings are accumulators of Cu (Tamari et al., 2014).

As plants usually take up Cu through their roots, the roots themselves must be tolerant or resistant to high Cu concentrations. This tolerance or resistance is maintained by biological processes in which functional proteins play an important role. In order to better understand the molecular mechanisms underlying Cu tolerance, proteomic studies have been performed using various roots exposed to excess Cu, including *Agrostis capillaris* L. (Hego et al., 2014),

Arabidopsis thaliana (L.) Heynh. (Kung et al., 2006), *Cannabis sativa* L. (Bona et al., 2007), *Elsholtzia splendens* Nakai (Liu et al., 2014), rice (*Oryza sativa* L.) (Chen et al., 2015; Song et al., 2013), and wheat (*Triticum aestivum* L.) (Li et al., 2013).

The aim of the present study was to understand how roots cope with Cu excess. We examined how Cu directly affects the propagation of cultured roots of *H. albus*, the locations to which Cu is allocated in the roots, and the biochemical and proteomic changes that are induced by Cu excess. In addition, we compared the proteome composition obtained in our previous study of *H. albus* roots subjected to Fe deficiency stress (Khandakar et al., 2013) and data reported in previous proteomic studies of other plant roots under Cu excess (Bona et al., 2007; Chen et al., 2015; Hego et al., 2014; Kung et al., 2006; Li et al., 2013) with the data from the present study to determine the novelty and/or generality of stress responses of *H. albus* roots.

2. Materials and Methods

2.1. Root materials and culture conditions

Root cultures of *H. albus* used in this study were established following Higa et al. (2008). Roots were maintained on MS basal medium (Murashige and Skoog, 1962) solidified with 0.2% (w/v) gellan gum. A primary root tip with a few lateral roots (approximately 2 cm in length), isolated from a 2-week-old root culture, was either directly cultured in test medium or pre-cultured in MS medium containing 1% (w/v) sucrose for 2 weeks and then transferred to test medium and cultured for 1 additional week. MS media containing different Cu concentrations (0, 0.1, 1, 20, and 200 μM), prepared by either elimination or addition of $CuSO_4$, were used as test media. $EDTANa_2$ (Doujindo Co., Japan), a chelating agent, was added to the 20 and 200 μM Cu media to prevent Cu precipitation. Media were autoclaved at 121 ºC for 15 min before use. All cultures were maintained in 100 mL and 50 mL conical flasks containing 25 mL and 15 mL of liquid medium, respectively, and incubated under agitation (80 rpm) at 25 ºC, in the dark. The cultures were harvested by vacuum filtration and washed with distilled water. Freshly collected roots were weighed and dried at 50 ºC overnight prior to analyses of root mass and amount of Cu in the roots (dry weight basis). Only fresh roots were used for fractionation analysis.

Following the protocol in a previous report for comparative proteomic analysis, root cultures were pre-propagated in B5 medium (Gamborg et al., 1968) containing 1% (w/v) sucrose for 2 weeks. Roots were then separated into sub-sets and transferred to fresh B5 medium containing 1% (w/v) sucrose, either with normal Cu concentration (0.1 μM) or with

high Cu concentration (200 μM). Root cultures were maintained for 5 days. Root tips were harvested at day 5, frozen in liquid nitrogen, and stored at -80 ºC until further use.

2.2. Proteomic analysis

Proteins were extracted from root tips (100 mg fresh weight) using bead beating followed by the acid guanidinium–phenol–chloroform method (Khandakar et al., 2013). The same methodological approach used in a previous small-scale proteomic analysis (Khandakar et al., 2013) was applied in the present study. In brief, 2-D gel electrophoresis (20 μg protein/2-D gel) was performed with a 7-cm ReadyStrip™ IPG Strip (73-mm-long, 3.3-mm-wide, and 0.5-mm-thick rehydrated strip with a linear pH gradient of 5–8; Bio-Rad, Hercules, CA, USA) for the 1st dimension and a Mini-PROTEAN® TGX™ gel AnykD (IPG/prep, 72-mm-long, 86-mm-wide, and 1-mm-thick gel; Bio-Rad) for the 2nd dimension. Gels were visualised with Flamingo® fluorescent staining (Bio-Rad). Image analysis, spot detection, statistical analysis, and protein in-gel digestion, followed by protein identification using matrix-assisted laser desorption/ionization quadrupole ion trap time-of-flight (MALDI-QIT-TOF) mass spectrometry and determination of *pI*, MW, and subcellular localisation were performed by following the methods described in our previous paper (Khandakar et al., 2013). Cross-species protein identification was performed by MS/MS ion search using MASCOT® version 2.3 (Matrix Science, London, UK). MS/MS spectra were processed with MASCOT Distiller™ version 2.3 (Matrix Science, London, UK), and resulting peak lists were searched against the SwissProt 2015_12 database (550,116 sequences and 196,219,159 residues; taxonomy: Viridiplantae, 37,197 sequences) and the EST_Solanaceae 2015_12 database (7,984,062 sequences and 1,484,673,610 residues) in our own MASCOT server. Search parameters were: trypsin (enzyme), carbamidomethyl (Cys; fixed modifications), oxidation (M; variable modifications), monoisotopic (mass values), ± 0.5 Da (peptide mass tolerance), ± 0.3 Da (fragment mass tolerance) and 1 (maximum missed cleavage). The identification was considered positive when the assigned MASCOT score was above threshold level ($p < 0.05$) (at least two peptides, protein score > 60; single peptide, peptide score > 48; annotated MS/MS spectra of the MASCOT peptide view are shown in Supplemental Data 1), sequence coverage was > 1.5%, and theoretical and observed mass and *pI* values were similar.

2.3. Fractionation

H. albus fresh root tissues (approximately 1 g) were fractionated according to the method reported previously (Tamari et al., 2014). Fresh weight (FW) of the cell-wall containing fraction

was measured after collection by nylon mesh filtration (82 μm, *in vacuo*) and washing twice with extraction buffer containing 50 mM Tris-HCl (pH 7.5), 250 mM sucrose, and 10 mM dithiothreitol. The sedimentation fractions, which included the nucleus plus plastid-rich and mitochondria-rich fractions, were isolated by centrifugation at 880 × *g* for 15 min, followed by 21,880 × *g* for 30 min. Their FWs were obtained by weighing empty centrifuge tubes, adding filtrate or supernatant to the tubes, and removing the supernatants after centrifugation. The tubes with sediments were again weighed, and the weights of the empty centrifuge tubes were subtracted from these values. FW of the remaining supernatant (considered as soluble fraction) was calculated by subtracting the weight of the sum of three fractions (the cell wall-containing fraction, the nucleus plus plastid-rich fraction, and the mitochondria-rich fraction) from that of the starting materials. The ratio (%) of FW in each fraction was calculated by dividing by the sum of FW in four fractions: the cell wall-containing fraction, the nucleus plus plastid rich-fraction, the mitochondria-rich fraction, and the soluble fraction. The ratio (%) of Cu amounts in each fraction was obtained in the same manner as that of FW.

2.4. Measurement of amount of Cu

Dried tissues and fractions were digested with 60% (w/v) HNO_3 in a microwave oven (Perkin Elmer Multiwave, MA, USA) at 160 ºC for 20 min. The amount of Cu was determined by atomic absorption spectroscopy (Hitachi Z-2000, Tokyo, Japan) based on a calibration curve prepared with a Cu standard solution (Wako Chemical, Osaka, Japan).

2.5. Assay of TTC-reducing activity

A 2,3,5-triphenyltetrazolium chloride (TTC)-reducing assay was used to determine respiration activity (Higa et al., 2010). Briefly, the medium was removed from the root culture using a pipette, roots were washed with 5 mL sterile water, and 10 mL filter-sterilised TTC reagent (Sigma) was added. The prepared TTC reagent was 0.5% (w/v) TTC in 50 mM potassium phosphate buffer (pH 7.0). Incubation with TTC reagent was performed under sterile conditions for 3 h with shaking (80 rpm) to allow the reagent to permeate uniformly.

After incubation, roots (50–150 mg) harvested by vacuum filtration were ground in liquid nitrogen to a powder with a mortar and a pestle. The powder was transferred to a centrifuge tube and extracted with 3 mL of 95% (v/v) ethanol for 15 min in a water bath at 60 ºC. After centrifugation (880 × *g*; 15 min), the absorbance of the supernatant was recorded at 520 nm. As the absorbance of denatured roots boiled for 10 min was 0.020 ± 0.001 at 520 nm, 95% (v/v) ethanol was used as control and 0.02 was subtracted from the absorbance value. Reduction activity was calculated using a standard curve previously obtained using authentic

1,3,5-triphenylformazan (Tokyo Chemical Industry Co., Tokyo, Japan) dissolved in 95% (v/v) ethanol.

2.6. Statistical analysis

All the experiments were performed using at least three replicates, and the means and standard deviations were calculated. The statistical differences were analysed by Student t-test or analysis of variance (ANOVA) using Excel Statistics software (Social Survey Research Information Co., Tokyo, Japan). Significant differences were expressed as $p < 0.05$ and $p < 0.01$.

3. Results

3.1. Effect of Cu concentration on root propagation

In order to establish the response of *H. albus* roots to Cu, root tips were inoculated into preparations of liquid MS media containing Cu at various concentrations (0.1, 1, 20, and 200 μM), as well as into Cu-free MS medium. Roots were then cultured for 7 and 14 days in the dark. Roots grew well at all Cu concentrations but not under the Cu-deficient condition. Root propagation was promoted at the highest Cu concentration. In particular, lateral root development was noticeably different at 200 μM Cu than at 0.1 μM, the normal Cu concentration (Fig. 1). Although there was no significant difference in the number of lateral roots, the length of these roots and particularly the distance from the main root tip to the first initiated lateral root differed significantly between treatments (Table 1). At 200 μM Cu, the distance from the main root tip was two-thirds that at 0.1 μM Cu. Root growth measured as dry weight (DW) was significantly suppressed under Cu-deficient conditions compared with that at 0.1 μM Cu (reduced from 5.9 ± 1.7 mg per culture to 2.3 ± 1.5 mg per culture after 14 days). However, after 14 days, root growth was enhanced when Cu was added, reaching the highest value at 200 μM Cu (11.6 ± 2.3 mg per culture) (Fig. 2). The effects of 200 μM Cu and Cu deficiency on root growth were also clearly seen after 7 days of culture, although the effects were not obvious at the other concentrations.

3.2. Cu accumulation in roots

As *H. albus* roots grew well under Cu-rich conditions (see section 3.1), root tissues cultured for 2 weeks in media containing 0.1, 20, or 200 μM Cu were analysed by atomic absorption

spectrometry. Cu accumulation increased with the increasing Cu concentration (Table 2). At a concentration of 200 μM Cu, the accumulation of Cu was about 14 times higher than that at the lowest concentration.

The bioaccumulation/bioconcentration factor (BF) has been proposed as a standard to estimate the ability of plants to take up arsenic from the rhizosphere (Masarovičová et al., 2010). In hydroponics, the ratio of metal concentration in plant dry mass ($\mu g.g^{-1}$ DW) to the external solution ($\mu g.cm^{-3}$) is used as a measure of BF. Our results showed that BF values of *H. albus* roots varied from 2,700 at the lowest Cu concentration to 19 at the highest.

The high levels of Cu incorporation into *H. albus* roots suggested that Cu might be accumulated at the subcellular level. To test whether this was occurring, root tissues were divided into four fractions by filtration and centrifugation: a cell wall-containing fraction, a fraction containing the nuclei plus plastids, a mitochondria-rich fraction, and a soluble fraction, including vacuoles and cytosol. Cu incorporation at 0.1 μM Cu occurred mostly in the cell-wall containing (approximately 39%) and soluble (approximately 37%) fractions, followed by the nucleus and plastid-rich fraction (approximately 13%) and the mitochondria-rich fraction (approximately 11%). At 200 μM Cu, Cu content increased in all fractions, but particularly in the cell wall-containing fraction (approximately 62%), followed by the soluble fraction (approximately 31%) (Table 3). The total amount of Cu recovered from the cell wall-containing fraction was more than 20 times as high for the 200 μM Cu treatment as for the 0.1 μM Cu concentration.

Interestingly, the calculation of the amount of Cu incorporated into each fraction relative to the fresh weight fraction (i.e. specific incorporation) showed that the highest specific incorporation was into the mitochondria-rich fraction, both at 0.1 μM and at 200 μM Cu. Moreover, the specific incorporation into this fraction increased over 16-fold between the 200 and the 0.1 μM Cu concentrations (Table 3). Relatively high specific incorporation of Cu into the nucleus and plastid-rich fraction was also observed.

3.3. Effect of Cu on root respiration

As root growth was enhanced by a concentration of 200 μM Cu (Fig. 2) and the mitochondria-rich fraction showed a high specific incorporation of Cu (Table 3), we anticipated that respiration activity would increase under conditions of Cu excess. To confirm whether this occurred, we examined the effect of Cu concentration (0.1 and 200 μM) on respiration activity, using the TTC-reducing assay. Results showed that respiration activity increased when the Cu concentration increased from 0.1 to 200 μM ($p < 0.05$) (Fig. 3), matching our predictions.

3.4. Protein profile under different Cu concentrations

In order to determine which proteins in *H. albus* roots were responsible for enhanced root propagation and higher Cu accumulation under Cu excess, comparative proteomic analysis was performed. Proteins were extracted from 100 mg fresh roots cultured in 0.1 and 200 μM Cu concentrations using CHAPS-urea solution. The total amount of soluble proteins in each treatment was not statistically different (Table 4). Two-dimensional gel electrophoresis of 20 μg of protein revealed more than 200 spots in each sample (Table 4, Fig. 4). Differential protein accumulation between the two Cu concentration treatments was analysed after normalisation using Prodigy SameSpots®, and a threshold value (ANOVA at $p < 0.05$) was set at ≥1.5-fold change. Thirty-four spots were detected, of which 21 increased and 13 decreased in abundance under Cu excess (Table 4).

These 34 spots were digested and peptides were extracted. Peptide solutions were then analysed by MALDI-QIT-TOF mass spectrometry. In total, 22 proteins were identified, of which 16 increased in abundance under Cu excess and the remainder decreased (Table 5; Supplemental Data 2). According to the previous classification based on their function (Khandakar et al., 2013), proteins were divided into five groups: carbohydrate metabolism (6 proteins, 27%), amino acid/protein metabolism (6 proteins, 27%), defence response (4 proteins, 18%), ATP-related metabolism (4 proteins, 18%), and other functions (2 proteins, 10%). Only 1 protein per group decreased in abundance under Cu excess and all the others increased, except in the defence response group, where 2 proteins decreased in abundance (Table 5).

Under Cu excess, 5 proteins involved in carbohydrate metabolism increased in abundance: 2 isozymes of pyrophosphate-fructose 6-phosphate and 1-phosphotransferase β-subunit (spots 13 and 74), enolase (spot 63) from the glycolytic pathway, NADP-dependent isocitrate dehydrogenase (ISD, spot 2), and a dihydrolipoamide dehydrogenase precursor (spot 17) from the TCA cycle. Also in this group, fructose-bisphosphate aldolase-like protein (spot 67) decreased in abundance. In the amino acid/protein metabolism group, 5 proteins increased in accumulation: ferredoxin-nitrite reductase (NiR, spot 4), which is responsible for assimilation of NO_2^-; the mitochondrial elongation factor Tu (EF-Tu) (spot 8), which is part of the mechanism that synthesises new proteins by translation at the ribosome; and 3 isozymes of *S*-adenosylmethionine (SAM) synthase (spots 6, 7 and 18), which catalyse the biosynthesis of SAM from methionine and ATP. The proteasome subunit β type-6 protein (spot 47), characterised by its ability to cleave peptides, decreased in abundance. Proteins related to ATP metabolism, such as the vacuolar H^+-ATPase A1 subunit isoform (spot 57), the ATP synthase

subunit α (spot 39), and the adenosine kinase (ADK) isoform (spot 9) increased in abundance, whereas the UMP/CMP kinase-like 1S (spot 46) decreased. Defence-response proteins that increased in abundance were the peroxidase 27 precursor putative (spot 1) and the heat shock cognate 70-kDa protein (HSP 70, spot 10), while the superoxide dismutase (SOD) [Fe] (spot 72) and the glutathione peroxidase (GPX, spot 61) decreased. Proteins belonging to the general group (other functions), such as the cell division control protein 48 homolog A (CDC, spot 12), which is involved in cell division and growth processes (Feiler et al., 1995), increased in abundance, but the soluble inorganic pyrophosphatase (PPA) decreased (spot 49). More than 2.0-fold increases in accumulation were observed in ISD (2.7-fold), peroxidase 27 (2.5-fold), NiR (2.2-fold), and vacuolar H^+-ATPase (2.1-fold).

4. Discussion

Supplying different concentrations of Cu (from 0 to 200 μM) to the roots of *H. albus* revealed that Cu deficiency causes serious growth impairment and Cu excess promotes root development (Table 1, Figs. 1 and 2), especially lateral root elongation, although it inhibits axis root elongation (Table 1, Fig. 1). Similar inhibition of axis root elongation, as well as enhancement of lateral root formation, in response to Cu excess was observed in *A. thaliana* (Lequeux et al., 2010; Potters et al., 2007; Wojcik and Tukiendorf, 2003). Meanwhile, lateral root length and total root weight sharply decreased under Cu excess, even at concentrations below 50 μM. Lateral elongation of *H. albus* roots was enhanced, and root weight also increased (Figs. 1 and 2, Table 1), indicating that roots thrive under Cu excess.

Comparative proteomic analysis revealed that, under conditions of Cu excess, cell division and *de novo* syntheses of amino acids and proteins were enhanced, whereas protein degradation was depressed, suggesting that the roots of *H. albus* actively grow when Cu is abundant. To support this active root growth, the energy supply in the roots was also enhanced, as shown by the increased accumulation of proteins involved in glycolysis, the TCA cycle, and the electron transport chain (ETC) (Table 5). These results coincided with the observed increase in respiration activity under Cu excess (Fig. 4). Cu excess may be involved in lateral root development either by activating hormones such as abscisic acid (ABA) (Gibson et al., 2012) or suppressing the production of new hormones such as strigolactones, which inhibit lateral root elongation. Although these results have been reported in *A. thaliana* (Kapulnik et al., 2011), the proteomic profile from the present study did not show support for these mechanisms in *H.*

albus.

Among the 22 proteins identified in this study, only 4 proteins (spots 1, 39, 49, and 61) were found in a previous proteomic analysis in *H. albus* roots subjected to Fe deficiency (Khandakar et al., 2013). Interestingly, soluble PPA (spot 49) and GPX (spot 61) decreased, and ATP synthase subunit α (spot 39) increased under Cu excess, whereas opposite results were obtained under Fe deficiency, except for the peroxidase 27 precursor putative (spot 1), which increased in both cases. Although *H. albus* roots are tolerant to Fe deficiency, they appear to respond with energetic and Fe-conservation strategies to severe Fe restriction. There may be a shift between *de novo* synthesis and enhanced reutilisation of amino acids produced by proteolysis (Khandakar et al., 2013). Under Cu excess, increased accumulations of ATP-involved proteins, including three SAM synthase isozymes (spots 6, 18, and 7), vacuolar H^+-ATPase (spot 57), ATP synthase subunit α (spot 39), ADK (spot 9), and CDC (spot 12), indicated active consumption and production of ATP. In addition, active *de novo* synthesis of amino acids and proteins seems to occur, as shown by the increased accumulation of NiR (spot 4) and mitochondrial EF-Tu (spot 8). Elevated levels of EF-Ts, the guanine nucleotide-exchange factor for EF-Tu, also occurred specifically in response to Cu in *Pseudomonas putida* Trevisan KT2440, suggesting that protein synthesis increases in response to Cu (Miller et al., 2009). In *Vibrio parahaemolyticus*, EF-Tu and EF-Ts were detected by secretomics and these proteins were abundant in strains that were tolerant to heavy metals (Cd and Cu) (He et al., 2015). On the other hand, proteolytic activity seems to decrease in the presence of heavy metals, as shown by the decrease in proteasome subunit (spot 47). A significant decrease in a proteasome was also observed in the marine brown algae *Sargassum fusiforme* (Harv.) Setchell when it was exposed to chronic Cu stress (Zou et al., 2015).

The proteomic profile of *H. albus* roots subjected to Cu excess was not consistent with previous results obtained using the roots of various plants (Bona et al., 2007; Hego et al., 2014; Li et al., 2013; Song et al., 2013). When the roots of wheat seedlings were exposed to 100 μM Cu, 3 proteins that are functionally similar to those found in *H. albus* roots were identified: HSP 70, SAM synthase 1, and ATP synthase α (Li et al., 2013). In wheat roots, HSP 70 and SAM synthase decreased, whereas in *H. albus* roots, both proteins increased. Nevertheless, the accumulation of ATP synthase increased in the roots of both species. In the roots of a Cu-tolerant rice variety exposed to 8 μM Cu (Song et al., 2013), SAM synthase and HSP 80 increased in abundance, similar to our observations in *H. albus*. *C. sativa* roots supplied with 600 μM Cu showed a decrease in enolase (Bona et al., 2007), while *H. albus* roots showed an increase in this protein. Likewise, enolase and ATP synthase α were reduced in roots of

metallicolous populations of *A. capillaris* in response to ~30 µM Cu (Hego et al., 2014), but opposite results were obtained in *H. albus* roots. These findings might be due to the different mechanisms used by different plant species to deal with excess Cu, the dose and period of Cu supply, or the age of plant materials.

H. albus roots actively accumulate Cu: the BF values of the roots varied between 2,700 (at 0.1 µM Cu) and 19 (at 200 µM Cu) (Table 2). BF values of excluders, accumulators, and hyperaccumulators are < 1, > 1, and > 10, respectively (Masarovičová et al., 2010). Therefore, *H. albus* roots take up Cu actively from the rhizosphere, especially at low Cu concentrations. Results suggest that *H. albus* roots need Cu for growth, an idea supported by the observations of severe growth impairment when the species is maintained under Cu-deficient conditions and of better root growth in the presence of excess Cu (Table 1, Figs. 1 and 2).

Cu accumulation in *H. albus* root cells occurred mainly in the cell-wall containing and the soluble fractions (Table 3). As vacuoles were included in the soluble fraction, these results seem consistent with the common response of plants to toxic metals. In bean (*Phaseolus vulgaris* L.) leaves, the cell wall was the major site of Cu ion accumulation (Bouazizi et al., 2011). Similarly, root cells of *Bechmeria nivea* (L.) Gaud. accumulated approximately 50% of total cadmium in the cell wall, followed by 37% in the soluble fraction (Wang et al., 2008). In the present study, the response to Cu excess (Table 3) was similar to the result in the *B. nivea* study; unlike previous studies, we used the roots of *H. albus* seedlings in which the soluble fraction contained higher amounts of Cu than the cell wall-containing fraction (Tamari et al., 2014). As cultured roots of *H. albus* are only able to transport Cu within root cells, Cu may be retained in apoplasts after it reaches saturation inside the cells. Vacuoles (classed as a soluble fraction) must be the main active site of Cu sequestration inside the cells, preventing Cu toxicity in the cytosol (Bernal et al., 2006). Membrane proteins that actively transport Cu, such as Cu-ATPases (Migocka, 2015) and copper transporter (Yu et al., 2014), could not be identified in the present study because only CHAPS-urea soluble proteins were analysed. Most proteins identified in this study exhibited negative values of GRAVY (grand average of hydropathy) (Table 5).

Vacuolar H^+-ATPase (spot 57) found in the present study seems to be linked to Cu accumulation in organelles such as vacuoles and mitochondria. Eide et al. (Eide et al., 1993) demonstrated that vacuolar H^+-ATPase was required for efficient Cu detoxification in *Saccharomyces cerevisiae*. This detoxification probably occurred in the vacuoles and the H^+-ATPase also probably played an important role in mitochondrial respiration. In *Vitis vinifera* L. cells, Cu compartmentation in the vacuole was dependent on the transmembrane pH gradient generated by vacuolar H^+-ATPase (Martins et al., 2012).

Recent proteomic analysis in *O. sativa* roots (Chen et al., 2015) and *A. thaliana* seedlings (Kung et al., 2006) exposed to excess Cu, using affinity chromatography, revealed that ADK, SAM, ISD, EF-2, and enolase are possible Cu-binding proteins. The enhanced accumulation of ADK, SAM, ISD, and enolase in *H. albus* roots subjected to Cu excess suggests that these proteins seem to function as Cu sinks in the cytoplasm.

A new finding of the present study is the notably high specific incorporation of Cu in the mitochondria that was observed in the 200 μM Cu treatment (Table 3). The mitochondrial respiratory component Complex IV (cytochrome *c* oxidase) contains two Cu centres and cytochromes as co-factors (Rasmusson and Browse, 2002). Therefore, an excess of Cu may result in the deposition of more Cu in Complex IV, which acts as a Cu sink. In fact, plastocyanin in the leaves of *A. thaliana* acts as a Cu sink when large amounts of Cu are available, in addition to its role as an electron carrier (Abdel-Ghany, 2009). In *H. albus* roots, increased accumulation of mitochondrial EF-Tu in response to Cu excess might facilitate the activation of Complex IV, as a consequence of protein synthesis activation in the mitochondria. In fact, respiration activity in *H. albus* root cultures was enhanced under Cu excess (Fig. 3).

Under Cu excess, many proteins involved in the defence response increased in *T. aestivum* (Li et al., 2013) and *O. sativa* (Chen et al., 2015; Song et al., 2013). This response was expected because an excess of Cu results in oxidative stress (Ravet and Pilon, 2013). However, in *H. albus* roots, increases were observed in peroxidase 27 (2.5-fold) and HSP 70 (1.5-fold), but decreases were seen in SOD [Fe] (-1.5-fold) and GPX (-1.5-fold). The function of peroxidase 27 is not yet known, but this protein increases under both Fe deficiency (Khandakar et al., 2013) and Cu excess (Table 5). It may become an important stress biomarker in *H. albus* roots.

5. Conclusions

H. albus seedlings tolerate excess Cu (Tamari et al., 2014). In the present study, *H. albus* roots, especially lateral roots, grew vigorously under Cu excess and accumulated large amounts of Cu. At the subcellular level, the total Cu amount was recovered mainly in the cell wall-containing fraction, followed by the soluble fraction, although the mitochondria-rich fraction contained the highest specific incorporation of Cu. This accumulation pattern may cause the enhanced respiration activity that was also observed. Our small-scale proteomic analysis revealed that active energy production and consumption, as well as an increase in protein synthesis (probably in the mitochondria) and cell division contributed to root growth under Cu excess. Many

proteins known to function as Cu-binding proteins and those that are candidates for this role, including the respiratory component Complex IV, ADK, SAM, ISD, and enolase, seem to function as Cu sinks. Newly propagated root tissues, including cell walls, cytoplasm, and intracellular compartments, in addition to functional proteins, such as Cu-binding proteins, provide further space and reservoirs for additional Cu deposition.

H. albus roots are tolerant to Fe deficiency and thrive under Cu excess. A comparison between this study and a previous small-scale proteomic analysis under Fe deficiency revealed that most proteins identified by the two studies differed, with the exception of 4 proteins, 3 of which show opposite behaviour in the two scenarios. Therefore, the biochemical mechanisms to tolerate Fe deficiency and to grow under Cu excess must be different. The uncharacterised protein peroxidase 27, which increased in both cases, may be used as a biomarker for the stress response. Further characterisation of peroxidase 27 may provide an insight into the mechanisms used by *H. albus* to cope with environmental stress.

Acknowledgements

We wish to thank all of the members of Prof. Tatsuya Oda's laboratory for their helpful cooperation on sample preparation for small-scale proteomics. We also thank Ms Mayumi Kudo for her technical assistance. This work was supported by a Grant-in-Aid (C, 24580479) from the Japan Society for the Promotion of Science.

476 **References**

477

478 Abdel-Ghany, S.E., 2009. Contribution of plastocyanin isoforms to photosynthesis and copper
479 homeostasis in *Arabidopsis thaliana* grown at different copper regimes. Planta 229, 767-779.

480 Bernal, M.A., Ramiro, M.V., Casesb, R., Picorel, R., Yruela, I., 2006. Excess copper effect on growth,
481 chloroplast ultrastructure, oxygen-evolution activity and chlorophyll fluorescence in *Glycine*
482 *max* cell suspensions. Physiol. Plant. 127, 312-325.

483 Bona, E., Marsano, F., Cavaletto, M., Berta, G., 2007. Proteomic characterization of copper stress
484 response in *Cannabis sativa* roots. Proteomics 7, 1121-1130.

485 Bouazizi, H., Jouili, H., Geitmann, A., El Ferjani, E., 2011. Cell wall accumulation of cu ions and
486 modulation of lignifying enzymes in primary leaves of bean seedlings exposed to excess copper.
487 Biol.Trace Elem. Res. 139, 97-107.

488 Burkhead, J.L., Reynolds, K.A., Abdel-Ghany, S.E., Cohu, C.M., Pilon, M., 2009. Copper homeostasis.
489 New Phytol. 182, 799-816.

490 Chen, C., Song, Y., Zhuang, K., Li, L., Xia, Y., Shen, Z., 2015. Proteomic analysis of copper-binding
491 proteins in excess copper-stressed roots of two rice (*Oryza sativa* L.) varieties with different Cu
492 tolerances. PLoS ONE 10, e0125367.

493 Eide, D.J., Bridgham, J.T., Zhao, Z., Mattoon, J.R., 1993. The vacuolar H+-ATPase of *Saccharomyces*
494 *cerevisiae* is required for efficient copper detoxification, mitochondrial function, and iron
495 metabolism. Mol. Gen. Genet. 241, 447-456.

496 Evans, W.C., 2009. Trease and Evans pharmacognosy, 16th ed. Saunders/Elsevier London, UK.

497 Feiler, H., Desprez, T., Santoni, V., Kronenberger, J., Caboche, M., Traas, J., 1995. The higher plant
498 *Arabidopsis thaliana* encodes a functional CDC48 homologue which is highly expressed in
499 dividing and expanding cells. EMBO J. 14, 5626-5637.

500 Gamborg, O.L., Miller, R.A., Ojima, K., 1968. Nutrient requirements of suspension cultures of soybean
501 root cells. Exp. Cell Res. 50, 151-158.

502 Gibson, S., Conway, A., Zheng, Z., Uchacz, T., Taylor, J., Todd, C., 2012. *Brassica carinata* CIL1
503 mediates extracellular ROS production during auxin- and ABA-regulated lateral root
504 development. J. Plant Biol. 55, 361-372.

505 He, Y., Wang, H., Chen, L., 2015. Comparative secretomics reveals novel virulence-associated factors of
506 *Vibrio parahaemolyticus*. Front. Microbiol. 6, 707.

507 Hego, E., Bes, C.M., Bedon, F., Palagi, P.M., Chaumeil, P., Barré, A., Claverol, S., Dupuy, J.W., Bonneu,
508 M., Lalanne, C., Plomion, C., Mench, M., 2014. Differential accumulation of soluble proteins in
509 roots of metallicolous and nonmetallicolous populations of *Agrostis capillaris* L. exposed to Cu.
510 Proteomics 14, 1746-1758.

511 Higa, A., Khandakar, J., Mori, Y., Kitamura, Y., 2012. Increased de novo riboflavin synthesis and
512 hydrolysis of FMN are involved in riboflavin secretion from *Hyoscyamus albus* hairy roots
513 under iron deficiency. Plant Physiol. Biochem. 58, 166-173.

514 Higa, A., Miyamoto, E., ur Rahman, L., Kitamura, Y., 2008. Root tip-dependent, active riboflavin
515 secretion by *Hyoscyamus albus* hairy roots under iron deficiency. Plant Physiol. Biochem. 46,
516 452-460.
517 Higa, A., Mori, Y., Kitamura, Y., 2010. Iron deficiency induces changes in riboflavin secretion and the
518 mitochondrial electron transport chain in hairy roots of *Hyoscyamus albus*. J. Plant Physiol. 167,
519 870-878.
520 Kapulnik, Y., Delaux, P.M., Resnick, N., Mayzlish-Gati, E., Wininger, S., Bhattacharya, C.,
521 Séjalon-Delmas, N., Combier, J.P., Bécard, G., Belausov, E., Beeckman, T., Dor, E.,
522 Hershenhorn, J., Koltai, H., 2011. Strigolactones affect lateral root formation and root-hair
523 elongation in *Arabidopsis*. Planta 233, 209-216.
524 Khandakar, J., Haraguchi, I., Yamaguchi, K., Kitamura, Y., 2013. A small-scale proteomic approach
525 reveals a survival strategy, including a reduction in alkaloid biosynthesis, in *Hyoscyamus albus*
526 roots subjected to iron deficiency. Front. Plant Sci. 4, 331.
527 Kung, C.C.S., Huang, W.N., Huang, Y.C., Yeh, K.C., 2006. Proteomic survey of copper‐binding proteins
528 in *Arabidopsis* roots by immobilized metal affinity chromatography and mass spectrometry.
529 Proteomics 6, 2746-2758.
530 Lequeux, H., Hermans, C., Lutts, S., Verbruggen, N., 2010. Response to copper excess in *Arabidopsis*
531 *thaliana*: Impact on the root system architecture, hormone distribution, lignin accumulation and
532 mineral profile. Plant Physiol. Biochem. 48, 673-682.
533 Li, G., Peng, X., Xuan, H., Wei, L., Yang, Y., Guo, T., Kang, G., 2013. Proteomic analysis of leaves and
534 roots of common wheat (*Triticum aestivum* L.) under copper-stress conditions. J. Proteome Res.
535 12, 4846-4861.
536 Liu, T., Shen, C., Wang, Y., Huang, C., Shi, J., 2014. New insights into regulation of proteome and
537 polysaccharide in cell wall of *Elsholtzia splendensin* response to copper stress. PLoS ONE 9,
538 e109573.
539 Martins, V., Hanana, M., Blumwald, E., Gerós, H., 2012. Copper transport and compartmentation in grape
540 cells. Plant Cell Physiol. 53, 1866-1880.
541 Masarovicˇova´, E., Kra´lˇova´, K., Kummerova, M., 2010. Principles of classification of medicinal
542 plants as hyperaccumulators or excluders. Acta Physiol. Plant. 32, 823-829.
543 Migocka, M., 2015. Copper-transporting ATPases: The evolutionarily conserved machineries for
544 balancing copper in living systems. IUBMB Life 67, 737-745.
545 Miller, C., Pettee, B., Zhang, C., Pabst, M., McLean, J., Anderson, A., 2009. Copper and cadmium:
546 responses in *Pseudomonas putida* KT2440. Lett. Appl. Microbiol. 49, 775-783.
547 Murashige, T., Skoog, F., 1962. A revised medium for rapid growth and bioassay with tobacco tissue
548 cultures. Physiol. Plant. 15, 473-497.
549 Potters, G., Pasternak, T.P., Guisez, Y., Palme, K.J., Jansen, M.A., 2007. Stress-induced morphogenic
550 responses: growing out of trouble? Trends Plant Sci. 12, 98-105.
551 Rasmusson, A., Browse, J., 2002. Respiration and lipid metabolism, in: Taiz, L., Zeiger, E. (Eds), Plant

552 Physiology. Sinauer Associates Inc., Massachusetts, pp. 223-258.
553 Ravet, K., Pilon, M., 2013. Copper and iron homeostasis in plants: The challenges of oxidative stress.
554 Antioxid. Redox Sign. 19, 919-932.
555 Sáez, C.A., Roncarati, F., Moenne, A., Moody, A.J., Brown, M.T., 2015. Copper-induced intra-specific
556 oxidative damage and antioxidant responses in strains of the brown alga *Ectocarpus siliculosus*
557 with different pollution histories. Aquat. Toxicol. 159, 81-89.
558 Song, Y., Cui, J., Zhang, H., Wang, G., Zhao, F.J., Shen, Z., 2013. Proteomic analysis of copper stress
559 responses in the roots of two rice (*Oryza sativa* L.) varieties differing in Cu tolerance. Plant Soil
560 366, 647-658.
561 Tamari, N., Mine, A., Sako, A., Tamagawa, S., Tabira, Y., Kitamura, Y., 2014. Possible application of the
562 medicinal plant *Hyoscyamus albus* in phytoremediation: Excess copper compensates for iron
563 deficiency, depending on the light conditions. Am. J. Plant Sci. 5, 3812-3822.
564 Visioli, G., Marmiroli, N., 2013. The proteomics of heavy metal hyperaccumulation by plants. J.
565 Proteomics 79, 133-145.
566 Wang, X., Liu, Y., Zeng, G., Chai, L., Song, X., Min, Z., Xiao, X., 2008. Subcellular distribution and
567 chemical forms of cadmium in *Bechmeria nivea* (L.) Gaud. Environ. Exp. Bot. 62, 389-395.
568 Terelak, H., Motowicka-Terelak, T., 2000. The heavy metals and sulphur status of agricultural soils in
569 Poland, in:Wilson, M., Maliszewska-Kordybach, B. (Eds), Soil quality, sustainable agriculture
570 and environmental security in Central and Eastern Europe. Springer Science & Business Media,
571 Dordrecht, pp. 37-48.
572 Wojcik, M., Tukiendorf, A., 2003. Response of wild type of *Arabidopsis thaliana* to copper stress. Biol.
573 Plantarum 46, 79-84.
574 Yu, P., Yuan, J., Deng, X., Ma, M., Zhang, H., 2014. Subcellular Targeting of Bacterial CusF Enhances Cu
575 Accumulation and Alters Root to Shoot Cu Translocation in *Arabidopsis*. Plant Cell Physiol. 55,
576 1568-1581.
577 Zou, H.-X., Pang, Q.-Y., Zhang, A.-Q., Lin, L.-D., Li, N., Yan, X.-F., 2015. Excess copper induced
578 proteomic changes in the marine brown algae *Sargassum fusiforme*. Ecotox. Environ. Safe. 111,
579 271-280.
580
581
582
583
584
585
586
587

588 **Figure Legends**

589

590 **Fig. 1** Morphological differences between roots cultured with 0.1 and 200 μM copper (Cu).
591 Root tips (approximately 2.0–2.5 cm) were cultured for 2 weeks in liquid Murashige
592 and Skoog medium. A bar indicates 1 cm.

593

594 **Fig. 2** Effects of various copper (Cu) concentrations on root mass.
595 Root tips (approximately 2.0–2.5 cm) were cultured for 1 and 2 weeks, respectively, in
596 liquid Murashige and Skoog medium without and with 0.1 to 200 μM Cu. n = 5. * and
597 ** indicate significant differences at the levels of $p < 0.05$ and $p < 0.01$ compared with
598 control (0.1 μM Cu).

599

600 **Fig. 3** Comparison of respiration activity in roots cultured with 0.1 and 200 μM copper (Cu).
601 Respiration activity was determined using the TTC-reducing assay. n = 3. * indicates a
602 significant difference at the levels of $p < 0.05$ compared with control (0.1 μM Cu).

603

604 **Fig. 4** 2-D gel protein profiles obtained from root tips cultured with 200 μM copper (Cu) (**A**)
605 and 0.1 μM Cu (**B**).
606 Proteins (20 μg) were separated on 7-cm IPG strips (pH 5–8 linear gradient) using
607 isoelectric focusing (IEF) in the first dimension, followed by AnykD® TGX™ gels in the
608 second dimension. Gels were visualised with Flamingo® fluorescent staining.
609 Differentially expressed spots were marked with arrows and numbers. The prodigy rank
610 number was used as a spot number (see Table 5). Molecular mass (kDa) and *pI* are
611 indicated on the left-hand and upper axes, respectively.

Fig. 1

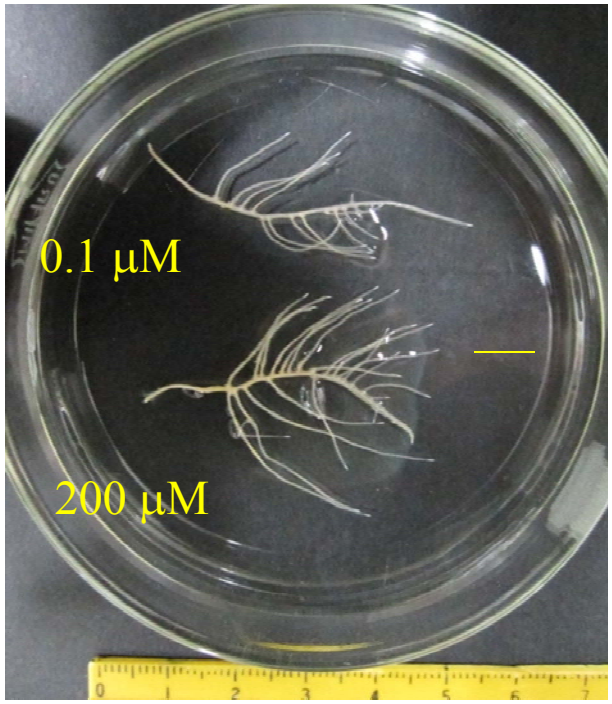

Fig. 2

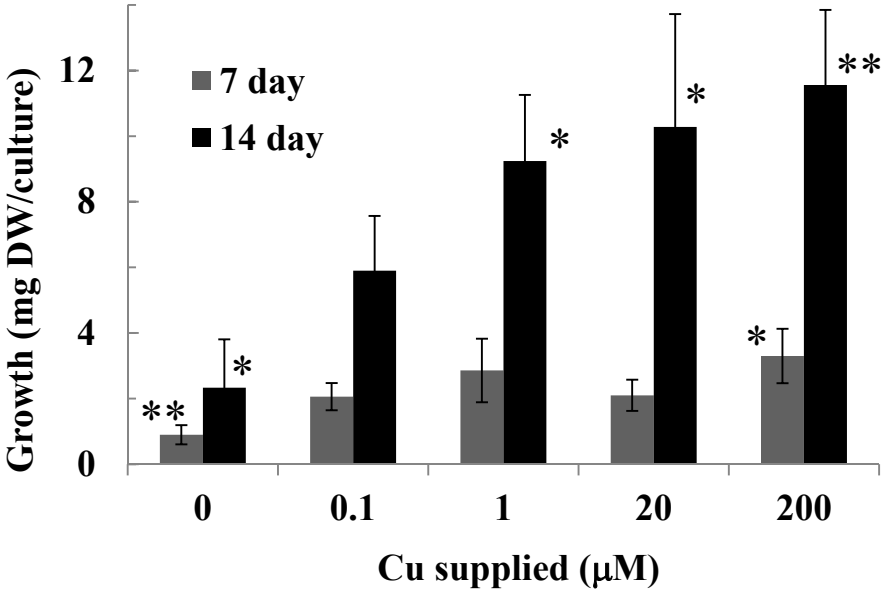
Growth (mg DW/culture)
12
8
4
0
7 day
14 day
**
*
*
*
*
**
0
0.1
1
20
200
Cu supplied (μM)

Fig. 3

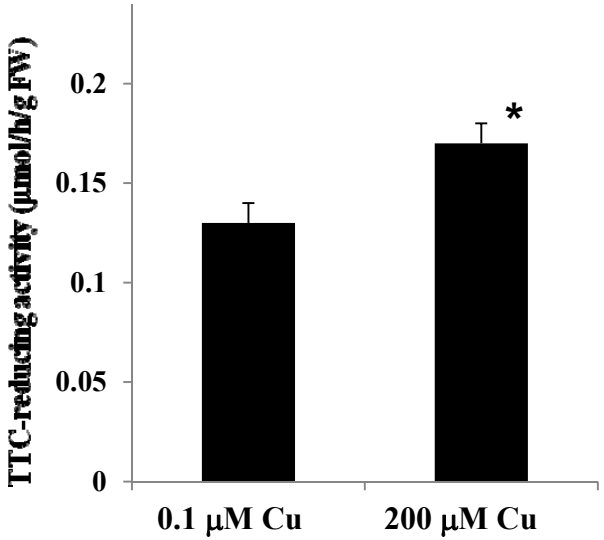
TTC-reducing activity (μmol/h/g FW)
0.2
0.15
0.1
0.05
0
*
0.1 μM Cu
200 μM Cu

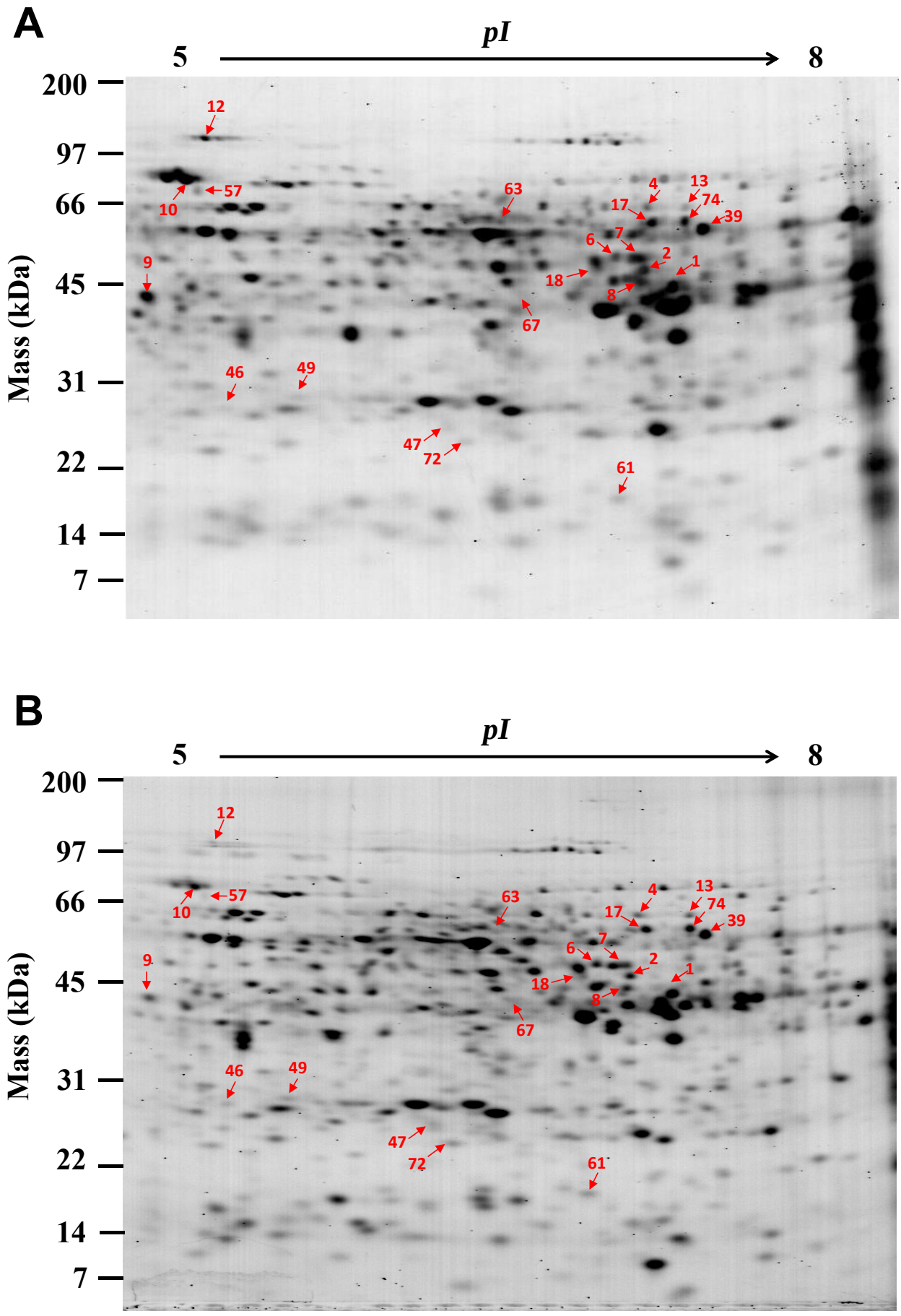
A
pI
5
8
200
97
66
45
31
22
14
7
Mass (kDa)
12
57
10
63
4
13
74
17
39
7
6
2
1
9
18
8
67
46
49
47
72
61
B
pI
5
8
200
97
66
45
31
22
14
7
Mass (kDa)
12
57
10
63
4
13
74
17
39
7
6
2
1
9
18
8
67
46
49
47
72
61

Table 1. Comparisons of lateral root developments in *Hyoscyamus albus* root cultures grown with different copper (Cu) concentrations

Determination	0.1 μM Cu	200 μM Cu
Number of lateral roots	14.4 ± 2.6	16.2 ± 3.6
Length of lateral root (mm)	14.5 ± 0.7	18.6 ± 1.0*
Distance from the main root tip to the first lateral root (mm)	14.4 ± 1.2	9.0 ± 1.2**

n = 12. * and ** indicate significant differences at the levels of $p < 0.05$ and $p < 0.01$ compared with control (0.1 μM Cu).

Table 2. Copper (Cu) accumulation in *Hyoscyamus albus* roots cultured in medium supplied with various Cu concentrations

Cu supply		Cu accumulation	
Concentration (μM)	Culture period (wks)	$\mu g.g^{-1}$ DW	BF*
0.1	2	17.1 ± 4.4	2700 ± 700
20	2	47.0 ± 0.6	37 ± 0.5
200	2	243.8 ± 49.5	19.2 ± 3.9

DW, dry weight. n = 3. * Bioaccumulation factor (BF) was calculated from the ratio of Cu concentration in root mass ($\mu g.\ g^{-1}$DW) to that in the culture medium ($\mu g.\ cm^{-3}$).

Table 3. Copper (Cu) distribution in various fractions from *Hyoscyamus albus* roots cultured with different Cu concentrations

Cu supply (μM)	Fractionation	g FW/culture	g FW (%)	Total Cu (nmol)	Total Cu (%)	Cu incorporation (nmol/g FFW)
0.1	Original roots used	1.138 ± 0.060				
	Cell walls [a)]	0.395 ± 0.145	34.7 ± 12.7	12.8 ± 2.7	39.4 ± 8.3	34.4 ± 8.4
	Nucleus and plastids [b)]	0.066 ± 0.013	5.8 ± 1.1	4.0 ± 0.7	12.5 ± 2.1	68.4 ± 14.0
	Mitochondria [c)]	0.032 ± 0.005	2.8 ± 0.4	3.5 ± 0.5	10.7 ± 1.6	110.8 ± 27.3
	Soluble fraction [d)]	0.645 ± 0.103	56.7 ± 9.1	12.1 ± 2.5	37.4 ± 7.6	19.4 ± 8.2
200	Original roots used	1.033 ± 0.218				
	Cell walls [a)]	0.517 ± 0.125	50.0 ± 12.1	279.2 ± 48.8	62.1 ± 10.9	545.5 ± 44.6
	Nucleus and plastids [b)]	0.022 ± 0.010	2.1 ± 0.9	15.7 ± 2.8	3.5 ± 0.6	539.3 ± 115.3
	Mitochondria [c)]	0.008 ± 0.001	0.8 ± 0.1	14.6 ± 4.6	3.2 ± 1.0	1787.5 ± 414.9
	Soluble fraction [d)]	0.486 ± 0.082	47.0 ± 7.9	140.45 ± 28.4	31.2 ± 6.3	294.6 ± 47.2

[a) ~ d):] Original roots were fractionated into 4 fractions; cell wall-containing fraction, nucleus and plastids-rich fraction, mitochondria-rich fraction, and soluble fraction. n = 3. FFW, fraction fresh weight.

Table 4. Comparisons of various proteomics associated parameters in *Hyoscyamus albus* root culture grown with differential copper (Cu) concentrations

Parameters	0.1 μM Cu	200 μM Cu
Root tips (mg FW)	100	100
Protein yields (mg protein.g^{-1}FW)	4.66 ± 0.37	5.03 ± 0.28
No. of spots detected	215 ± 4	202 ± 2
No. of spots changed (≧1.5-fold) on 2D gels*	34	
(increased in relative abundance)		(21)
(decreased in relative abundance)		(13)
No. of protein spots identified	22	
(increased in relative abundance)		(16)
(decreased in relative abundance)		(6)

A 20 μg volume of proteins was separated on small gels (7 cm x 7 cm). * To analyse differential protein accumulation between the two conditions of Cu availability, a threshold value (ANOVA at $p < 0.05$) was set at ≧1.5-fold change after normalisation using Prodigy SameSpots®.

Table 5. MS/MS-based cross-species identification and characterization of the protein spots that showed significant volume increase (upper column) and decrease (lower column), respectively, under Cu excess condition.

Spot No.	Protein Name	Species	Accession No. (NCBI)	Theoretical Mass (kDa)/*pI*	Observed Mass (kDa)/*pI*	PS[a]	NMP[a]	SC[b] (%)	Fold (Cu2000/Cu1)	Subcellular Localization[c]	GRAVY[d]
《significant increase under high-copper conditions》↑											
CARBOHYDRATE METABOLISM											
2	Isocitrate dehydrogenase [NADP]	*Solanum tuberosum*	P50217	46.79/6.54	48.2/7.0	131	3	8	2.7	Cytoplasm	-0.307
13	Pyrophosphate-fructose 6-phosphate 1-phosphotransferasebeta-subunit	*Solanum tuberosum*	NP_001275324	56.49/6.21	62.4/7.2	61	2	5	1.8	Plastid or Mitochondria	-0.122
63	Enolase	*Solanum lycopersicum*	P26300	47.80/5.68	58.5/6.5	64	1[f]	3	1.6	Cytoplasm	-0.234
74	Pyrophosphate-fructose 6-phosphate 1-phosphotransferasebeta-subunit	*Solanum tuberosum*	NP_001275324	56.49/6.21	59.3/7.2	67	2	6	1.5	Plastid or Mitochondria	-0.122
17	Dihydrolipoamide dehydrogenase precursor	*Solanum tuberosum*	NP_001275339	53.41/6.41	59.3/7.0	77	1[f]	4	1.5	Mitochondria	0.02
AMINO ACID/PROTEIN METABOLISM											
4	Ferredoxin-nitrite reductase	*Arabidopsis thaliana*	Q39161	65.50/5.95	62.4/7.0	70	2	4	2.2	Plastid	-0.396
8	Elongation factor Tu, mitochondrial	*Arabidopsis thaliana*	Q9ZT91	49.41/6.25	45.2/7.0	144	3	9	1.7	Mitochondria	-0.178
6	S-adenosylmethionine synthase	*Pinus banksiana*	P50300	43.17/5.53	50.7/6.9	52	1[f]	4	1.5	Cytoplasm	-0.334
18	S-adenosylmethionine synthase 2	*Solanum tuberosum*	Q38JH8	42.70/5.67	48.2/6.8	102	2	7	1.5	Cytoplasm	-0.284
7	S-adenosylmethionine synthase	*Brassica rapa*	Q5DNB1	43.18/5.67	50.7/7.0	113	2	8	1.5	Cytoplasm	-0.334
DEFENSE RESPONSE											
1[e]	Peroxidase 27 precursor putative	*Ricinus communis*	XP_002280216	35.67/8.89	46.9/7.1	52	1	5	2.5	Secreted	-0.036
10	Heat shock cognate 70 kDa protein	*Petunia x hybrida*	P09189	71.23/5.10	73.9/5.2	141	3	7	1.5	Cytoplasm	-0.421
ETC/ATP INVOLVED REACTION											
57	Vacuolar H+-ATPase A1 subunit isoform	*Solanum lycopersicum*	NP_001234281	68.57/5.20	69.3/5.3	58	1[f]	7	2.1	Cytoplasm	-0.164
39[e]	ATP Synthase subunit alpha	*Arabidopsis thaliana*	P92549	55.05/6.23	57.0/7.2	61	2	8	1.5	Mitochondria	-0.029
9	Adenosine kinase isoform 1S	*Nicotiana tabacum*	AAU14832	37.44/5.07	44.6/5.1	49	1[f]	5	1.5	Cytoplasm	-0.187
OTHERS											
12	Cell division control protein 48 homolog A	*Arabidopsis thaliana*	P54609	59.39/5.13	87.5/5.3	61	1[f]	2	1.8	Cytoplasm	-0.381
Spot No.	Protein Name	Species	Accession No. (NCBI)	Theoretical Mass (kDa)/*pI*	Observed Mass (kDa)/*pI*	PS[a]	NMP[a]	SC[b] (%)	Fold (Cu1/Cu2000)	Subcellular Localization[c]	GRAVY[d]
《significant decrease under high-copper conditions》↓											
CARBOHYDRATE METABOLISM											
67	Fructose-bisphosphate aldolase-like protein	*Solanum tuberosum*	NP_001275379	38.62/7.51	46.3/6.6	55	1[f]	6	1.6	Cytoplasm	-0.228
AMINO ACID/PROTEIN METABOLISM											
47	Proteasome subunit beta type-6	*Arabidopsis thaliana*	Q8LD27	25.15/5.31	21.9/6.3	99	2	14	1.5	Cytoplasm or Nucleus	-0.095
DEFENSE RESPONSE											
72	Superoxide dismutase [Fe]	*Nicotiana plumbaginifoli*	P22302	23.04/5.53	23.6/6.3	63	2	9	1.6	Plastid	-0.392
61[e]	Glutathione peroxidase	*Solanum lycopersicum*	NP_001234567	18.84/6.58	18.2/6.9	89	3	21	1.5	Secreted	-0.394
ETC/ATP INVOLVED REACTION											
46	Predicted UMP/CMP kinase-like	*Solanum lycopersicum*	XP_004229700	22.87/5.76	27.2/5.4	83	2	14	1.5	Cytoplasm	-0.277
OTHERS											
49[e]	Soluble inorganic phosphsphatase	*Solanum tuberosum*	Q43187	24.26/5.59	29.0/5.7	58	1	8	1.5	Cytoplasm	-0.45

[a] Protein score (PS) and number of matched peptide (NMP) were obtained from Mascot search.

[b] Percentage of sequence coverage (SC) of identified peptides related to the corresponding sequence in database.

[c] Predicted by WOLF PSORT program using corresponding ORF (in the indicated accession number) as the query sequence.

[d] GRAVY (the grand average of hydropathy) values were calculated with ProtParam tool (see Materials and Methods).

[e] Corresponds to the same spot position and spot number as identified by Khandakar et al. (2013).

[f] Annotated MS/MS spectra are provided in Supplemental data.

Spot 63. Enolase

Peptide View

MS/MS Fragmentation of **IEEELGSEAVYAGASFR**
Found in **ENO_SOLLC**, Enolase OS=Solanum lycopersicum GN=PGH1 PE=2 SV=1

Match to Query 1: 1826.715724 from(1827.723000,1+)
Title: 1: Scan 1 (rt=0, well=E1)
Data file tempfile

Click mouse within plot area to zoom in by factor of two about that point
Or, Plot from 300 to 1900 Da Full range
Label all possible matches ○ Label matches used for scoring ◉

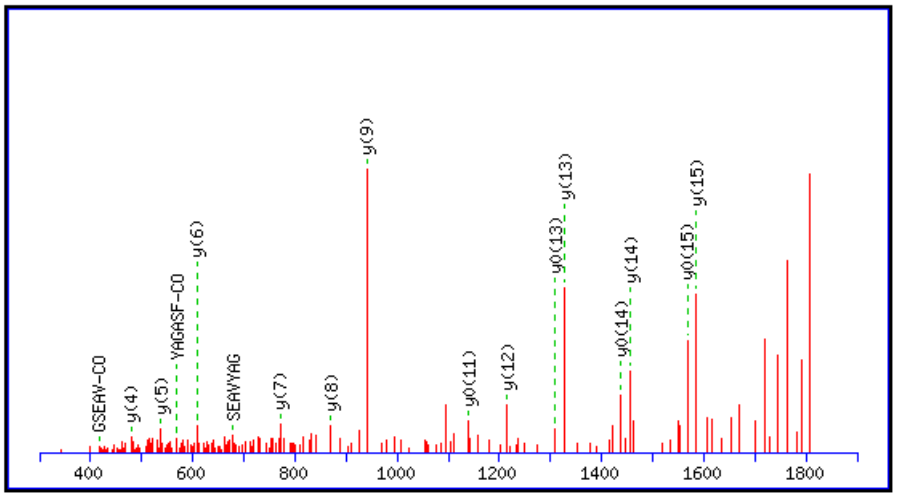

Monoisotopic mass of neutral peptide Mr(calc): 1826.8686
Fixed modifications: Carbamidomethyl (C) (apply to specified residues or termini only)
Ions Score: 64 **Expect:** 2.1e-005
Matches : 18/259 fragment ions using 30 most intense peaks (help)

#	Immon.	a	a^0	b	b^0	Seq.	y	y*	y^0	#
1	86.0964	86.0964		114.0913		I				17
2	102.0550	215.1390	197.1285	243.1339	225.1234	E	1714.7919	1697.7653	1696.7813	16
3	102.0550	344.1816	326.1710	372.1765	354.1660	E	*1585.7493*	1568.7227	1567.7387	15
4	102.0550	473.2242	455.2136	501.2191	483.2086	E	*1456.7067*	1439.6801	1438.6961	14
5	86.0964	586.3083	568.2977	614.3032	596.2926	L	*1327.6641*	1310.6375	1309.6535	13
6	30.0338	643.3297	625.3192	671.3246	653.3141	G	*1214.5800*	1197.5535	1196.5695	12
7	60.0444	730.3618	712.3512	758.3567	740.3461	S	1157.5586	1140.5320	1139.5480	11
8	102.0550	859.4044	841.3938	887.3993	869.3887	E	1070.5265	1053.5000	1052.5160	10
9	44.0495	930.4415	912.4309	958.4364	940.4258	A	*941.4839*	924.4574	923.4734	9
10	72.0808	1029.5099	1011.4993	1057.5048	1039.4942	V	*870.4468*	853.4203	852.4363	8
11	136.0757	1192.5732	1174.5626	1220.5681	1202.5576	Y	*771.3784*	754.3519	753.3679	7
12	44.0495	1263.6103	1245.5998	1291.6052	1273.5947	A	*608.3151*	591.2885	590.3045	6
13	30.0338	1320.6318	1302.6212	1348.6267	1330.6161	G	*537.2780*	520.2514	519.2674	5
14	44.0495	1391.6689	1373.6583	1419.6638	1401.6533	A	*480.2565*	463.2300	462.2459	4
15	60.0444	1478.7009	1460.6904	1506.6958	1488.6853	S	409.2194	392.1928	391.2088	3
16	120.0808	1625.7693	1607.7588	1653.7643	1635.7537	F	322.1874	305.1608		2
17	129.1135					R	175.1190	158.0924		1

Spot 63. Enolase (continued)

Seq	ya	yb	Seq	ya	yb	Seq	ya	yb
EE	231.0975	259.0925	EEE	360.1401	388.1351	EEEL	473.2242	501.2191
EEELG	530.2457	558.2406	EEELGS	617.2777	645.2726	EE	231.0975	259.0925
EEL	344.1816	372.1765	EELG	401.2031	429.1980	EELGS	488.2351	516.2300
EELGSE	617.2777	645.2726	EELGSEA	688.3148	716.3097	EL	215.1390	243.1339
ELG	272.1605	300.1554	ELGS	359.1925	387.1874	ELGSE	488.2351	516.2300
ELGSEA	559.2722	587.2671	ELGSEAV	658.3406	686.3355	LG	143.1179	171.1128
LGS	230.1499	258.1448	LGSE	359.1925	387.1874	LGSEA	430.2296	458.2245
LGSEAV	529.2980	557.2930	LGSEAVY	692.3614	720.3563	GS	117.0659	145.0608
GSE	246.1084	274.1034	GSEA	317.1456	345.1405	GSEAV	416.2140	444.2089
GSEAVY	579.2773	607.2722	GSEAVYA	650.3144	678.3093	SE	189.0870	217.0819
SEA	260.1241	288.1190	SEAV	359.1925	387.1874	SEAVY	522.2558	550.2508
SEAVYA	593.2930	621.2879	SEAVYAG	650.3144	678.3093	EA	173.0921	201.0870
EAV	272.1605	300.1554	EAVY	435.2238	463.2187	EAVYA	506.2609	534.2558
EAVYAG	563.2824	591.2773	EAVYAGA	634.3195	662.3144	AV	143.1179	171.1128
AVY	306.1812	334.1761	AVYA	377.2183	405.2132	AVYAG	434.2398	462.2347
AVYAGA	505.2769	533.2718	AVYAGAS	592.3089	620.3039	VY	235.1441	263.1390
VYA	306.1812	334.1761	VYAG	363.2027	391.1976	VYAGA	434.2398	462.2347
VYAGAS	521.2718	549.2667	VYAGASF	668.3402	696.3352	YA	207.1128	235.1077
YAG	264.1343	292.1292	YAGA	335.1714	363.1663	YAGAS	422.2034	450.1983
YAGASF	569.2718	597.2667	AG	101.0709	129.0659	AGA	172.1081	200.1030
AGAS	259.1401	287.1350	AGASF	406.2085	434.2034	GA	101.0709	129.0659
GAS	188.1030	216.0979	GASF	335.1714	363.1663	AS	131.0815	159.0764
ASF	278.1499	306.1448	SF	207.1128	235.1077			

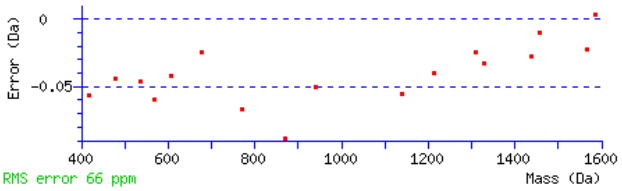

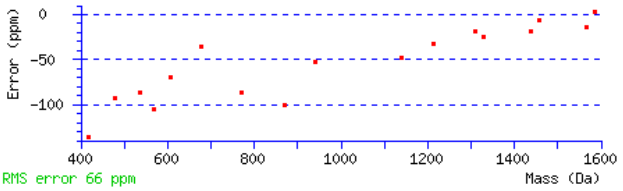

Spot 67. Fructose-bisphosphate aldolase-like protein

Peptide View

MS/MS Fragmentation of **IGANEPSQLAINENANGLAR**
Found in **gil25014723**, KS09020F02 KS09 Capsicum annuum cDNA, mRNA sequence
Translated in frame 3 (nucleic acid sequence)

Match to Query 1: 2051.272724 from(2052.280000,1+)
Title: 1: Scan 1 (rt=0, well=F2)
Data file tempfile

Click mouse within plot area to zoom in by factor of two about that point
Or, Plot from 400 to 2100 Da Full range
Label all possible matches ○ Label matches used for scoring ◉

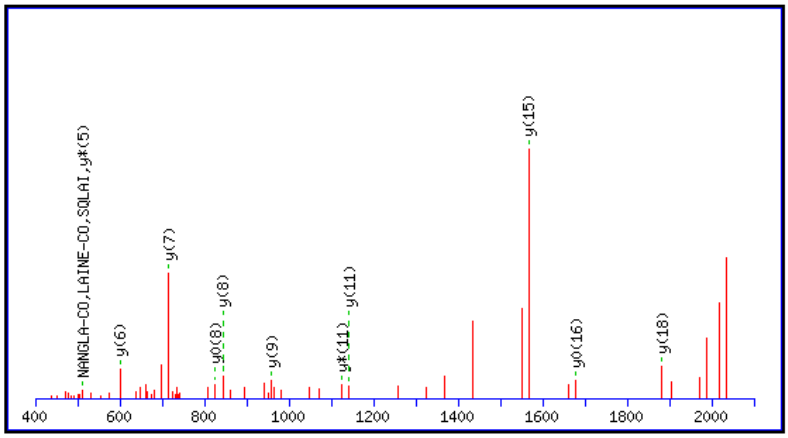

Monoisotopic mass of neutral peptide Mr(calc): 2051.0395
Fixed modifications: Carbamidomethyl (C) (apply to specified residues or termini only)
Ions Score: 55 **Expect:** 0.0095
Matches : 14/329 fragment ions using 14 most intense peaks (help)

#	Immon.	a	a*	a^0	b	b*	b^0	Seq.	y	y*	y^0	#
1	86.0964	86.0964			114.0913			I				20
2	30.0338	143.1179			171.1128			G	1938.9628	1921.9362	1920.9522	19
3	44.0495	214.1550			242.1499			A	***1881.9413***	1864.9148	1863.9308	18
4	87.0553	328.1979	311.1714		356.1928	339.1663		N	1810.9042	1793.8777	1792.8936	17
5	102.0550	457.2405	440.2140	439.2300	485.2354	468.2089	467.2249	E	1696.8613	1679.8347	1678.8507	16
6	70.0651	554.2933	537.2667	536.2827	582.2882	565.2617	564.2776	P	***1567.8187***	1550.7921	1549.8081	15
7	60.0444	641.3253	624.2988	623.3148	669.3202	652.2937	651.3097	S	1470.7659	1453.7394	1452.7554	14
8	101.0709	769.3839	752.3573	751.3733	797.3788	780.3523	779.3682	Q	1383.7339	1366.7074	1365.7233	13
9	86.0964	882.4680	865.4414	864.4574	910.4629	893.4363	892.4523	L	1255.6753	1238.6488	1237.6648	12
10	44.0495	953.5051	936.4785	935.4945	981.5000	964.4734	963.4894	A	***1142.5913***	1125.5647	1124.5807	11
11	86.0964	1066.5891	1049.5626	1048.5786	1094.5840	1077.5575	1076.5735	I	1071.5541	1054.5276	1053.5436	10
12	87.0553	1180.6321	1163.6055	1162.6215	1208.6270	1191.6004	1190.6164	N	***958.4701***	941.4435	940.4595	9
13	102.0550	1309.6747	1292.6481	1291.6641	1337.6696	1320.6430	1319.6590	E	***844.4272***	827.4006	826.4166	8
14	87.0553	1423.7176	1406.6910	1405.7070	1451.7125	1434.6859	1433.7019	N	***715.3846***	698.3580		7
15	44.0495	1494.7547	1477.7281	1476.7441	1522.7496	1505.7231	1504.7390	A	***601.3416***	584.3151		6
16	87.0553	1608.7976	1591.7711	1590.7871	1636.7925	1619.7660	1618.7820	N	530.3045	513.2780		5
17	30.0338	1665.8191	1648.7925	1647.8085	1693.8140	1676.7875	1675.8034	G	416.2616	399.2350		4
18	86.0964	1778.9032	1761.8766	1760.8926	1806.8981	1789.8715	1788.8875	L	359.2401	342.2136		3
19	44.0495	1849.9403	1832.9137	1831.9297	1877.9352	1860.9086	1859.9246	A	246.1561	229.1295		2
20	129.1135							R	175.1190	158.0924		1

Spot 67. Fructose-bisphosphate aldolase-like protein (continued)

Seq	ya	yb	Seq	ya	yb	Seq	ya	yb
GA	101.0709	129.0659	GAN	215.1139	243.1088	GANE	344.1565	372.1514
GANEP	441.2092	469.2041	GANEPS	528.2413	556.2362	GANEPSQ	656.2998	684.2947
AN	158.0924	186.0873	ANE	287.1350	315.1299	ANEP	384.1878	412.1827
ANEPS	471.2198	499.2147	ANEPSQ	599.2784	627.2733	NE	216.0979	244.0928
NEP	313.1506	341.1456	NEPS	400.1827	428.1776	NEPSQ	528.2413	556.2362
NEPSQL	641.3253	669.3202	EP	199.1077	227.1026	EPS	286.1397	314.1347
EPSQ	414.1983	442.1932	EPSQL	527.2824	555.2773	EPSQLA	598.3195	626.3144
PS	157.0972	185.0921	PSQ	285.1557	313.1506	PSQL	398.2398	426.2347
PSQLA	469.2769	497.2718	PSQLAI	582.3610	610.3559	PSQLAIN	696.4039	724.3988
SQ	188.1030	216.0979	SQL	301.1870	329.1819	SQLA	372.2241	400.2191
SQLAI	485.3082	513.3031	SQLAIN	599.3511	627.3461	QL	214.1550	242.1499
QLA	285.1921	313.1870	QLAI	398.2762	426.2711	QLAIN	512.3191	540.3140
QLAINE	641.3617	669.3566	LA	157.1335	185.1285	LAI	270.2176	298.2125
LAIN	384.2605	412.2554	LAINE	513.3031	541.2980	LAINEN	627.3460	655.3410
LAINENA	698.3832	726.3781	AI	157.1335	185.1285	AIN	271.1765	299.1714
AINE	400.2191	428.2140	AINEN	514.2620	542.2569	AINENA	585.2991	613.2940
AINENAN	699.3420	727.3369	IN	200.1394	228.1343	INE	329.1819	357.1769
INEN	443.2249	471.2198	INENA	514.2620	542.2569	INENAN	628.3049	656.2998
INENANG	685.3264	713.3213	NE	216.0979	244.0928	NEN	330.1408	358.1357
NENA	401.1779	429.1728	NENAN	515.2208	543.2158	NENANG	572.2423	600.2372
NENANGL	685.3264	713.3213	EN	216.0979	244.0928	ENA	287.1350	315.1299
ENAN	401.1779	429.1728	ENANG	458.1994	486.1943	ENANGL	571.2834	599.2784
ENANGLA	642.3206	670.3155	NA	158.0924	186.0873	NAN	272.1353	300.1302
NANG	329.1568	357.1517	NANGL	442.2409	470.2358	NANGLA	513.2780	541.2729
AN	158.0924	186.0873	ANG	215.1139	243.1088	ANGL	328.1979	356.1928
ANGLA	399.2350	427.2300	NG	144.0768	172.0717	NGL	257.1608	285.1557
NGLA	328.1979	356.1928	GL	143.1179	171.1128	GLA	214.1550	242.1499
LA	157.1335	185.1285						

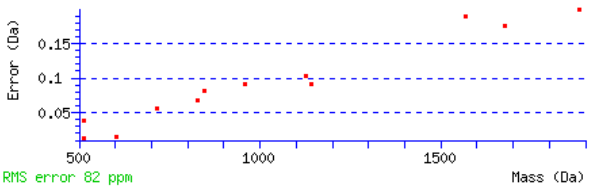

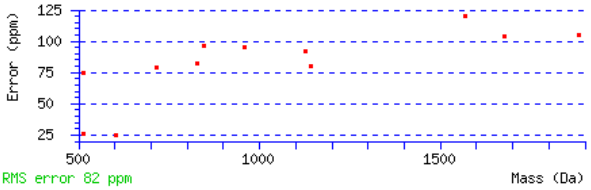

Spot 17. Dihydrolipoamide dehydrogenase precursor

Peptide View

MS/MS Fragmentation of **FLSPSEISVDTVEGGNSVVK**
Found in **gil5894612**, EST282165 tomato callus, TAMU Solanum lycopersicum cDNA clone cLEC36P6, mRNA sequence
Translated in frame 2 (nucleic acid sequence)

Match to Query 1: 2063.347724 from(2064.355000,1+)
Title: 1: Scan 1 (rt=0, well=F9)
Data file tempfile

Click mouse within plot area to zoom in by factor of two about that point
Or, Plot from 300 to 2100 Da Full range
Label all possible matches ○ Label matches used for scoring ◉

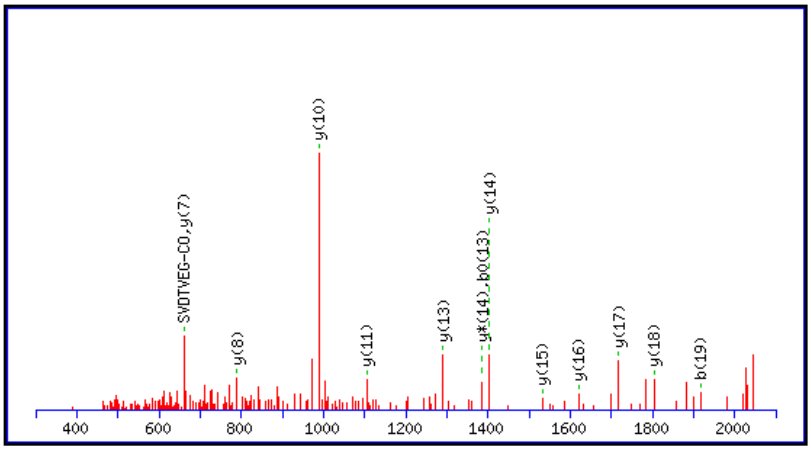

Monoisotopic mass of neutral peptide Mr(calc): 2063.0423
Fixed modifications: Carbamidomethyl (C) (apply to specified residues or termini only)
Ions Score: 77 **Expect:** 7.4e-005
Matches : 14/318 fragment ions using 17 most intense peaks (help)

#	Immon.	a	a*	a^0	b	b*	b^0	Seq.	y	y*	y^0	#
1	120.0808	120.0808			148.0757			F				20
2	86.0964	233.1648			261.1598			L	1916.9811	1899.9546	1898.9706	19
3	60.0444	320.1969		302.1863	348.1918		330.1812	S	*1803.8971*	1786.8705	1785.8865	18
4	70.0651	417.2496		399.2391	445.2445		427.2340	P	*1716.8650*	1699.8385	1698.8545	17
5	60.0444	504.2817		486.2711	532.2766		514.2660	S	*1619.8123*	1602.7857	1601.8017	16
6	102.0550	633.3243		615.3137	661.3192		643.3086	E	*1532.7802*	1515.7537	1514.7697	15
7	86.0964	746.4083		728.3978	774.4032		756.3927	I	*1403.7377*	1386.7111	1385.7271	14
8	60.0444	833.4403		815.4298	861.4353		843.4247	S	*1290.6536*	1273.6270	1272.6430	13
9	72.0808	932.5088		914.4982	960.5037		942.4931	V	1203.6216	1186.5950	1185.6110	12
10	88.0393	1047.5357		1029.5251	1075.5306		1057.5201	D	*1104.5531*	1087.5266	1086.5426	11
11	74.0600	1148.5834		1130.5728	1176.5783		1158.5677	T	*989.5262*	972.4997	971.5156	10
12	72.0808	1247.6518		1229.6412	1275.6467		1257.6361	V	888.4785	871.4520	870.4680	9
13	102.0550	1376.6944		1358.6838	1404.6893		1386.6787	E	*789.4101*	772.3836	771.3995	8
14	30.0338	1433.7159		1415.7053	1461.7108		1443.7002	G	*660.3675*	643.3410	642.3570	7
15	30.0338	1490.7373		1472.7267	1518.7322		1500.7217	G	603.3461	586.3195	585.3355	6
16	87.0553	1604.7802	1587.7537	1586.7697	1632.7752	1615.7486	1614.7646	N	546.3246	529.2980	528.3140	5
17	60.0444	1691.8123	1674.7857	1673.8017	1719.8072	1702.7806	1701.7966	S	432.2817	415.2551	414.2711	4
18	72.0808	1790.8807	1773.8541	1772.8701	1818.8756	1801.8491	1800.8650	V	345.2496	328.2231		3
19	72.0808	1889.9491	1872.9225	1871.9385	1917.9440	1900.9175	1899.9334	V	246.1812	229.1547		2
20	101.1073							K	147.1128	130.0863		1

Spot 17. Dihydrolipoamide dehydrogenase precursor (continued)

Seq	ya	yb	Seq	ya	yb	Seq	ya	yb
LS	173.1285	201.1234	LSP	270.1812	298.1761	LSPS	357.2132	385.2082
LSPSE	486.2558	514.2508	LSPSEI	599.3399	627.3348	LSPSEIS	686.3719	714.3668
SP	157.0972	185.0921	SPS	244.1292	272.1241	SPSE	373.1718	401.1667
SPSEI	486.2558	514.2508	SPSEIS	573.2879	601.2828	SPSEISV	672.3563	700.3512
PS	157.0972	185.0921	PSE	286.1397	314.1347	PSEI	399.2238	427.2187
PSEIS	486.2558	514.2508	PSEISV	585.3243	613.3192	SE	189.0870	217.0819
SEI	302.1710	330.1660	SEIS	389.2031	417.1980	SEISV	488.2715	516.2664
SEISVD	603.2984	631.2933	EI	215.1390	243.1339	EIS	302.1710	330.1660
EISV	401.2395	429.2344	EISVD	516.2664	544.2613	EISVDT	617.3141	645.3090
IS	173.1285	201.1234	ISV	272.1969	300.1918	ISVD	387.2238	415.2187
ISVDT	488.2715	516.2664	ISVDTV	587.3399	615.3348	SV	159.1128	187.1077
SVD	274.1397	302.1347	SVDT	375.1874	403.1823	SVDTV	474.2558	502.2508
SVDTVE	603.2984	631.2933	SVDTVEG	660.3199	688.3148	VD	187.1077	215.1026
VDT	288.1554	316.1503	VDTV	387.2238	415.2187	VDTVE	516.2664	544.2613
VDTVEG	573.2879	601.2828	VDTVEGG	630.3093	658.3042	DT	189.0870	217.0819
DTV	288.1554	316.1503	DTVE	417.1980	445.1929	DTVEG	474.2195	502.2144
DTVEGG	531.2409	559.2358	DTVEGGN	645.2838	673.2788	TV	173.1285	201.1234
TVE	302.1710	330.1660	TVEG	359.1925	387.1874	TVEGG	416.2140	444.2089
TVEGGN	530.2569	558.2518	TVEGGNS	617.2889	645.2838	VE	201.1234	229.1183
VEG	258.1448	286.1397	VEGG	315.1663	343.1612	VEGGN	429.2092	457.2041
VEGGNS	516.2413	544.2362	VEGGNSV	615.3097	643.3046	EG	159.0764	187.0713
EGG	216.0979	244.0928	EGGN	330.1408	358.1357	EGGNS	417.1728	445.1678
EGGNSV	516.2413	544.2362	EGGNSVV	615.3097	643.3046	GG	87.0553	115.0502
GGN	201.0982	229.0931	GGNS	288.1302	316.1252	GGNSV	387.1987	415.1936
GGNSVV	486.2671	514.2620	GN	144.0768	172.0717	GNS	231.1088	259.1037
GNSV	330.1772	358.1721	GNSVV	429.2456	457.2405	NS	174.0873	202.0822
NSV	273.1557	301.1506	NSVV	372.2241	400.2191	SV	159.1128	187.1077
SVV	258.1812	286.1761	VV	171.1492	199.1441			

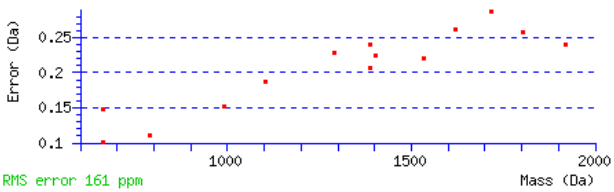

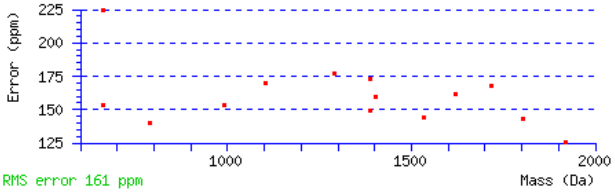

Spot 6. S-adenosylmethionine synthase

Peptide View

MS/MS Fragmentation of **YLDENTIFHLNPSGR**
Found in **METK_PINBN**, S-adenosylmethionine synthase OS=Pinus banksiana GN=METK PE=2 SV=1

Match to Query 1: 1774.462724 from(1775.470000,1+)
Title: 1: Scan 1 (rt=0, well=A12)
Data file tempfile

Click mouse within plot area to zoom in by factor of two about that point
Or, Plot from 300 to 1800 Da Full range
Label all possible matches ○ Label matches used for scoring ◉

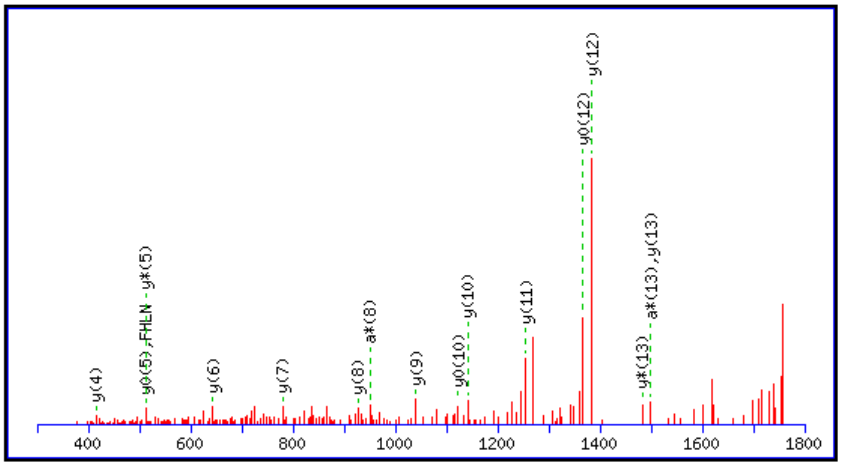

Monoisotopic mass of neutral peptide Mr(calc): 1774.8638
Fixed modifications: Carbamidomethyl (C) (apply to specified residues or termini only)
Ions Score: 52 **Expect:** 0.00034
Matches : 17/221 fragment ions using 28 most intense peaks (help)

#	Immon.	a	a*	a^0	b	b*	b^0	Seq.	y	y*	y^0	#
1	136.0757	136.0757			164.0706			Y				15
2	86.0964	249.1598			277.1547			L	1612.8078	1595.7812	1594.7972	14
3	88.0393	364.1867		346.1761	392.1816		374.1710	D	*1499.7237*	1482.6972	1481.7132	13
4	102.0550	493.2293		475.2187	521.2242		503.2136	E	*1384.6968*	1367.6702	1366.6862	12
5	87.0553	607.2722	590.2457	589.2617	635.2671	618.2406	617.2566	N	*1255.6542*	1238.6276	1237.6436	11
6	74.0600	708.3199	691.2933	690.3093	736.3148	719.2883	718.3042	T	*1141.6113*	1124.5847	1123.6007	10
7	86.0964	821.4040	804.3774	803.3934	849.3989	832.3723	831.3883	I	*1040.5636*	1023.5370	1022.5530	9
8	120.0808	968.4724	951.4458	950.4618	996.4673	979.4407	978.4567	F	*927.4795*	910.4530	909.4690	8
9	110.0713	1105.5313	1088.5047	1087.5207	1133.5262	1116.4997	1115.5156	H	*780.4111*	763.3846	762.4005	7
10	86.0964	1218.6154	1201.5888	1200.6048	1246.6103	1229.5837	1228.5997	L	*643.3522*	626.3256	625.3416	6
11	87.0553	1332.6583	1315.6317	1314.6477	1360.6532	1343.6266	1342.6426	N	530.2681	513.2416	512.2576	5
12	70.0651	1429.7110	1412.6845	1411.7005	1457.7060	1440.6794	1439.6954	P	*416.2252*	399.1987	398.2146	4
13	60.0444	1516.7431	1499.7165	1498.7325	1544.7380	1527.7114	1526.7274	S	319.1724	302.1459	301.1619	3
14	30.0338	1573.7645	1556.7380	1555.7540	1601.7594	1584.7329	1583.7489	G	232.1404	215.1139		2
15	129.1135							R	175.1190	158.0924		1

Spot 6. S-adenosylmethionine synthase (continued)

Seq	ya	yb	Seq	ya	yb	Seq	ya	yb
LD	201.1234	229.1183	LDE	330.1660	358.1609	LDEN	444.2089	472.2038
LDENT	545.2566	573.2515	LDENTI	658.3406	686.3355	DE	217.0819	245.0768
DEN	331.1248	359.1197	DENT	432.1725	460.1674	DENTI	545.2566	573.2515
DENTIF	692.3250	720.3199	EN	216.0979	244.0928	ENT	317.1456	345.1405
ENTI	430.2296	458.2245	ENTIF	577.2980	605.2930	NT	188.1030	216.0979
NTI	301.1870	329.1819	NTIF	448.2554	476.2504	NTIFH	585.3144	613.3093
NTIFHL	698.3984	726.3933	TI	187.1441	215.1390	TIF	334.2125	362.2074
TIFH	471.2714	499.2663	TIFHL	584.3555	612.3504	TIFHLN	698.3984	726.3933
IF	233.1648	261.1598	IFH	370.2238	398.2187	IFHL	483.3078	511.3027
IFHLN	597.3507	625.3457	IFHLNP	694.4035	722.3984	FH	257.1397	285.1346
FHL	370.2238	398.2187	FHLN	484.2667	512.2616	FHLNP	581.3194	609.3144
FHLNPS	668.3515	696.3464	HL	223.1553	251.1503	HLN	337.1983	365.1932
HLNP	434.2510	462.2459	HLNPS	521.2831	549.2780	HLNPSG	578.3045	606.2994
LN	200.1394	228.1343	LNP	297.1921	325.1870	LNPS	384.2241	412.2191
LNPSG	441.2456	469.2405	NP	184.1081	212.1030	NPS	271.1401	299.1350
NPSG	328.1615	356.1565	PS	157.0972	185.0921	PSG	214.1186	242.1135
SG	117.0659	145.0608						

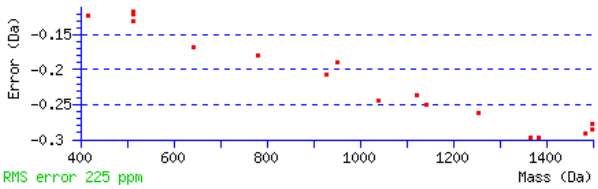

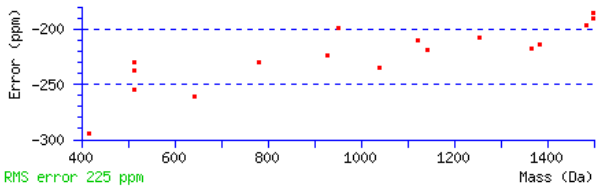

Spot 57. Vacuolar H^+−ATPase A1 subunit isoform

Peptide View

MS/MS Fragmentation of **LHDDLIAGFR**
Found in **gil224682944**, KS18003A11 KS18 Capsicum annuum cDNA, mRNA sequence
Translated in frame 2 (nucleic acid sequence)

Match to Query 1: 1155.593676 from(1156.600952,1+)
Title: "Ha2_MS2_[1156.615]_0001"
Data file Automatically uploaded data

Click mouse within plot area to zoom in by factor of two about that point
Or, Plot from 300 to 1150 Da Full range
Label all possible matches ○ Label matches used for scoring ◉

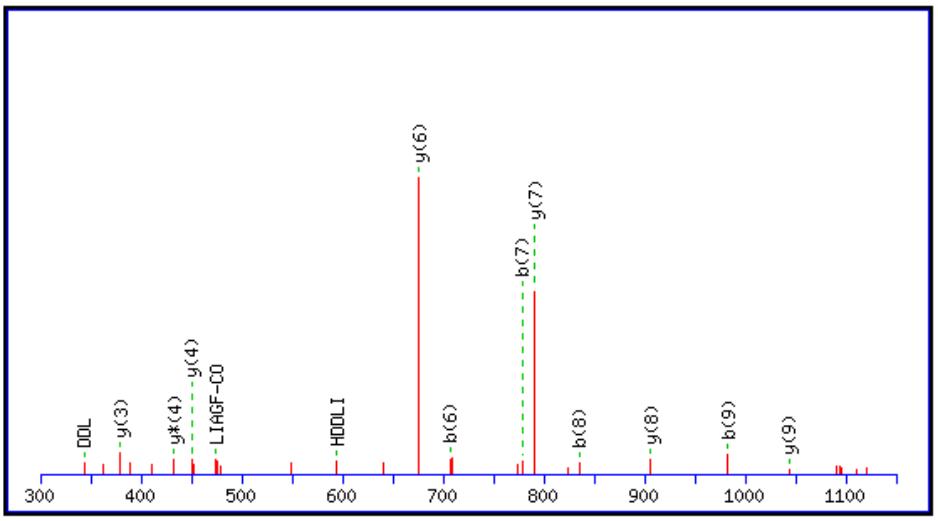

Monoisotopic mass of neutral peptide Mr(calc): 1155.6037
Fixed modifications: Carbamidomethyl (C) (apply to specified residues or termini only)
Ions Score: 58 **Expect:** 0.013
Matches : 15/114 fragment ions using 21 most intense peaks (help)

#	Immon.	a	a^0	b	b^0	Seq.	y	y*	y^0	#
1	86.0964	86.0964		114.0913		L				10
2	110.0713	223.1553		251.1503		H	*1043.5269*	1026.5003	1025.5163	9
3	88.0393	338.1823	320.1717	366.1772	348.1666	D	*906.4680*	889.4414	888.4574	8
4	88.0393	453.2092	435.1987	481.2041	463.1936	D	*791.4410*	774.4145	773.4305	7
5	86.0964	566.2933	548.2827	*594.2882*	576.2776	L	*676.4141*	659.3875		6
6	86.0964	679.3774	661.3668	*707.3723*	689.3617	I	563.3300	546.3035		5
7	44.0495	750.4145	732.4039	*778.4094*	760.3988	A	*450.2459*	433.2194		4
8	30.0338	807.4359	789.4254	*835.4308*	817.4203	G	*379.2088*	362.1823		3
9	120.0808	954.5043	936.4938	*982.4993*	964.4887	F	322.1874	305.1608		2
10	129.1135					R	175.1190	158.0924		1

Spot 57. Vacuolar H^+–ATPase A1 subunit isoform (continued)

Seq	ya	yb	Seq	ya	yb	Seq	ya	yb
HD	225.0982	253.0931	HDD	340.1252	368.1201	HDDL	453.2092	481.2041
HDDLI	566.2933	594.2882	HDDLIA	637.3304	665.3253	HDDLIAG	694.3519	722.3468
DD	203.0662	231.0612	DDL	316.1503	344.1452	DDLI	429.2344	457.2293
DDLIA	500.2715	528.2664	DDLIAG	557.2930	585.2879	DL	201.1234	229.1183
DLI	314.2074	342.2023	DLIA	385.2445	413.2395	DLIAG	442.2660	470.2609
DLIAGF	589.3344	617.3293	LI	199.1805	227.1754	LIA	270.2176	298.2125
LIAG	327.2391	355.2340	LIAGF	474.3075	502.3024	IA	157.1335	185.1285
IAG	214.1550	242.1499	IAGF	361.2234	389.2183	AG	101.0709	129.0659
AGF	248.1394	276.1343	GF	177.1022	205.0972			

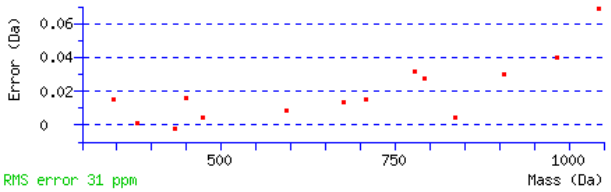

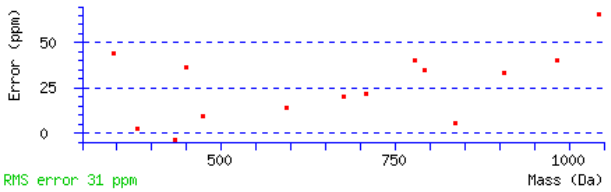

Spot 9. Adenosine kinase isoform 1S

Peptide View

MS/MS Fragmentation of **ALPYMDFVFGNETEAR**
Found in **gi|15186292**, 183A01 Mature tuber lambda ZAP Solanum tuberosum cDNA, mRNA sequence
Translated in frame 3 (nucleic acid sequence)

Match to Query 1: 1875.122724 from(1876.130000,1+)
Title: 1: Scan 1 (rt=0, well=M9)
Data file tempfile

Click mouse within plot area to zoom in by factor of two about that point
Or, Plot from 100 to 1900 Da Full range
Label all possible matches ○ Label matches used for scoring ◉

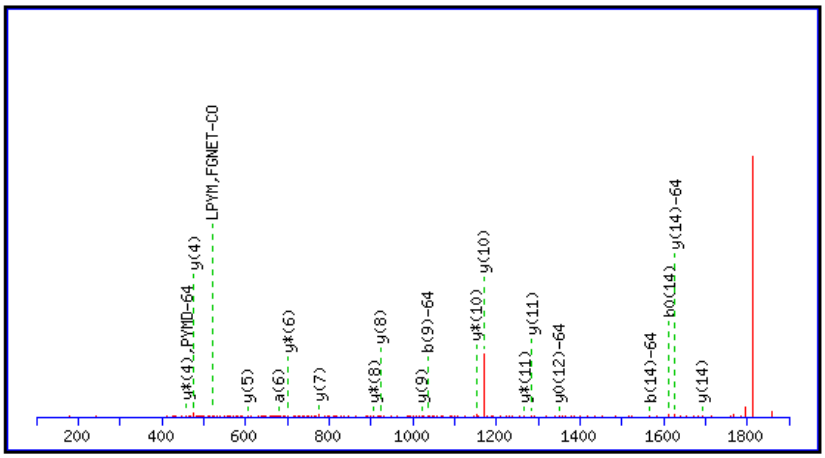

Monoisotopic mass of neutral peptide Mr(calc): 1874.8509
Fixed modifications: Carbamidomethyl (C) (apply to specified residues or termini only)
Variable modifications:
M5 : Oxidation (M), with neutral losses 63.9983(shown in table), 0.0000
Ions Score: 49 **Expect:** 0.047
Matches : 22/320 fragment ions using 32 most intense peaks (help)

#	Immon.	a	a*	a^0	b	b*	b^0	Seq.	y	y*	y^0	#
1	44.0495	44.0495			72.0444			A				16
2	86.0964	157.1335			185.1285			L	1740.8228	1723.7962	1722.8122	15
3	70.0651	254.1863			282.1812			P	*1627.7387*	1610.7122	1609.7281	14
4	136.0757	417.2496			445.2445			Y	1530.6860	1513.6594	1512.6754	13
5	56.0495	500.2867			528.2817			M	1367.6226	1350.5961	1349.6121	12
6	88.0393	615.3137		597.3031	643.3086		625.2980	D	*1284.5855*	1267.5590	1266.5749	11
7	120.0808	762.3821		744.3715	790.3770		772.3665	F	*1169.5586*	1152.5320	1151.5480	10
8	72.0808	861.4505		843.4400	889.4454		871.4349	V	*1022.4901*	1005.4636	1004.4796	9
9	120.0808	1008.5189		990.5084	**1036.5138**		1018.5033	F	*923.4217*	906.3952	905.4112	8
10	30.0338	1065.5404		1047.5298	1093.5353		1075.5247	G	*776.3533*	759.3268	758.3428	7
11	87.0553	1179.5833	1162.5568	1161.5728	1207.5782	1190.5517	1189.5677	N	719.3319	702.3053	701.3213	6
12	102.0550	1308.6259	1291.5994	1290.6154	1336.6208	1319.5943	1318.6103	E	*605.2889*	588.2624	587.2784	5
13	74.0600	1409.6736	1392.6470	1391.6630	1437.6685	1420.6420	1419.6579	T	*476.2463*	459.2198	458.2358	4
14	102.0550	1538.7162	1521.6896	1520.7056	**1566.7111**	1549.6846	1548.7005	E	375.1987	358.1721	357.1881	3
15	44.0495	1609.7533	1592.7268	1591.7427	1637.7482	1620.7217	1619.7377	A	246.1561	229.1295		2
16	129.1135							R	175.1190	158.0924		1

Spot 9. Adenosine kinase isoform 1S (continued)

Seq	ya	yb	Seq	ya	yb	Seq	ya	yb
LP	183.1492	211.1441	LPY	346.2125	374.2074	LPYM	429.2496	457.2445
LPYMD	544.2766	572.2715	LPYMDF	691.3450	719.3399	PY	233.1285	261.1234
PYM	316.1656	344.1605	PYMD	431.1925	459.1874	PYMDF	578.2609	606.2558
PYMDFV	677.3293	705.3243	YM	219.1128	247.1077	YMD	334.1397	362.1347
YMDF	481.2082	509.2031	YMDFV	580.2766	608.2715	MD	171.0764	199.0713
MDF	318.1448	346.1397	MDFV	417.2132	445.2082	MDFVF	564.2817	592.2766
MDFVFG	621.3031	649.2980	DF	235.1077	263.1026	DFV	334.1761	362.1710
DFVF	481.2445	509.2395	DFVFG	538.2660	566.2609	DFVFGN	652.3089	680.3039
FV	219.1492	247.1441	FVF	366.2176	394.2125	FVFG	423.2391	451.2340
FVFGN	537.2820	565.2769	FVFGNE	666.3246	694.3195	VF	219.1492	247.1441
VFG	276.1707	304.1656	VFGN	390.2136	418.2085	VFGNE	519.2562	547.2511
VFGNET	620.3039	648.2988	FG	177.1022	205.0972	FGN	291.1452	319.1401
FGNE	420.1878	448.1827	FGNET	521.2354	549.2304	FGNETE	650.2780	678.2729
GN	144.0768	172.0717	GNE	273.1193	301.1143	GNET	374.1670	402.1619
GNETE	503.2096	531.2045	GNETEA	574.2467	602.2416	NE	216.0979	244.0928
NET	317.1456	345.1405	NETE	446.1882	474.1831	NETEA	517.2253	545.2202
ET	203.1026	231.0975	ETE	332.1452	360.1401	ETEA	403.1823	431.1773
TE	203.1026	231.0975	TEA	274.1397	302.1347	EA	173.0921	201.0870

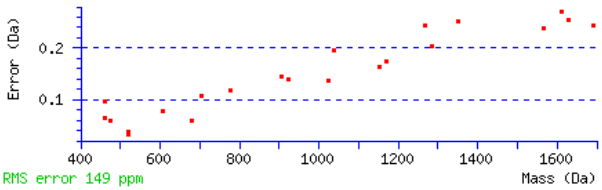

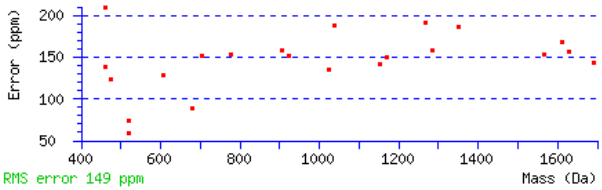

Spot 12. Cell division control protein 48 homolog A

Peptide View

MS/MS Fragmentation of **KYQAFAQTLQQSR**
Found in **CD48A_ARATH**, Cell division control protein 48 homolog A OS=Arabidopsis thaliana GN=CDC48A PE=1 SV=1

Match to Query 1: 1568.053724 from(1569.061000,1+)
Title: 1: Scan 1 (rt=0, well=F5)
Data file tempfile

Click mouse within plot area to zoom in by factor of two about that point
Or, Plot from 200 to 1600 Da Full range
Label all possible matches ○ Label matches used for scoring ◉

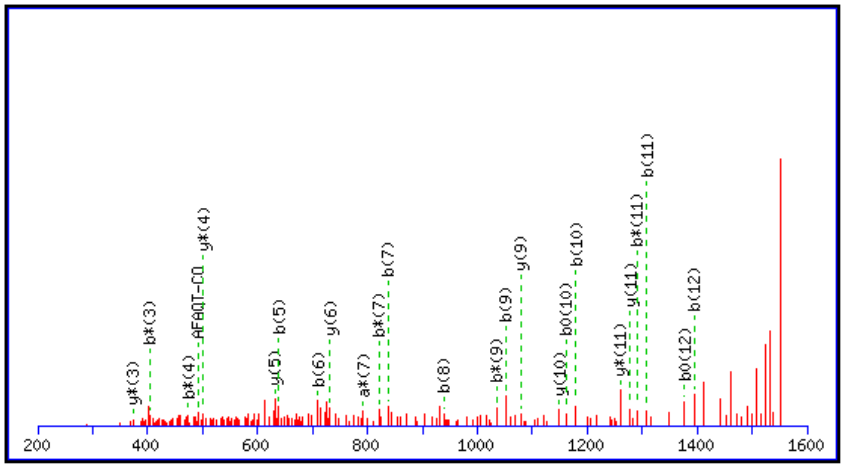

Monoisotopic mass of neutral peptide Mr(calc): 1567.8107
Fixed modifications: Carbamidomethyl (C) (apply to specified residues or termini only)
Ions Score: 61 **Expect:** 4.6e-005
Matches : 26/185 fragment ions using 39 most intense peaks (help)

#	Immon.	a	a*	a^0	b	b*	b^0	Seq.	y	y*	y^0	#
1	101.1073	101.1073	84.0808		129.1022	112.0757		K				13
2	136.0757	264.1707	247.1441		292.1656	275.1390		Y	1440.7230	1423.6965	1422.7124	12
3	101.0709	392.2292	375.2027		420.2241	403.1976		Q	**1277.6597**	1260.6331	1259.6491	11
4	44.0495	463.2663	446.2398		***491.2613***	474.2347		A	**1149.6011**	1132.5746	1131.5905	10
5	120.0808	610.3348	593.3082		***638.3297***	621.3031		F	**1078.5640**	1061.5374	1060.5534	9
6	44.0495	681.3719	664.3453		***709.3668***	692.3402		A	931.4956	914.4690	913.4850	8
7	101.0709	809.4305	792.4039		***837.4254***	820.3988		Q	860.4585	843.4319	842.4479	7
8	74.0600	910.4781	893.4516	892.4676	***938.4730***	921.4465	920.4625	T	**732.3999**	715.3733	714.3893	6
9	86.0964	1023.5622	1006.5356	1005.5516	***1051.5571***	1034.5306	1033.5465	L	**631.3522**	614.3257	613.3416	5
10	101.0709	1151.6208	1134.5942	1133.6102	***1179.6157***	1162.5891	1161.6051	Q	518.2681	501.2416	500.2576	4
11	101.0709	1279.6794	1262.6528	1261.6688	***1307.6743***	1290.6477	1289.6637	Q	390.2096	373.1830	372.1990	3
12	60.0444	1366.7114	1349.6848	1348.7008	***1394.7063***	1377.6797	1376.6957	S	262.1510	245.1244	244.1404	2
13	129.1135							R	175.1190	158.0924		1

Spot 12. Cell division control protein 48 homolog A (continued)

Seq	ya	yb	Seq	ya	yb	Seq	ya	yb
YQ	264.1343	292.1292	YQA	335.1714	363.1663	YQAF	482.2398	510.2347
YQAFA	553.2769	581.2718	YQAFAQ	681.3355	709.3304	QA	172.1081	200.1030
QAF	319.1765	347.1714	QAFA	390.2136	418.2085	QAFAQ	518.2722	546.2671
QAFAQT	619.3198	647.3148	AF	191.1179	219.1128	AFA	262.1550	290.1499
AFAQ	390.2136	418.2085	AFAQT	491.2613	519.2562	AFAQTL	604.3453	632.3402
FA	191.1179	219.1128	FAQ	319.1765	347.1714	FAQT	420.2241	448.2191
FAQTL	533.3082	561.3031	FAQTLQ	661.3668	689.3617	AQ	172.1081	200.1030
AQT	273.1557	301.1506	AQTL	386.2398	414.2347	AQTLQ	514.2984	542.2933
AQTLQQ	642.3570	670.3519	QT	202.1186	230.1135	QTL	315.2027	343.1976
QTLQ	443.2613	471.2562	QTLQQ	571.3198	599.3148	QTLQQS	658.3519	686.3468
TL	187.1441	215.1390	TLQ	315.2027	343.1976	TLQQ	443.2613	471.2562
TLQQS	530.2933	558.2882	LQ	214.1550	242.1499	LQQ	342.2136	370.2085
LQQS	429.2456	457.2405	QQ	229.1295	257.1244	QQS	316.1615	344.1565
QS	188.1030	216.0979						

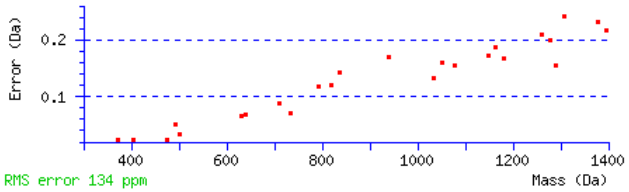

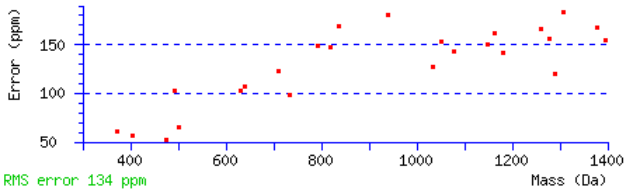

Supplementary Data 2. Results of MS/MS ion search and BLAST search for protein identification.

Spot No[a]	Protein ID	EST (Accession No.)[b]	Homolog (Accession No.)[c]	Species[d]	m/z	Sequence[e]	Delta	Miss[f]	Score	Expect
CARBOHYDRATE METABOLISM										
2	Isocitrate dehydrogenase [NADP]	ND	IDHC_SOLTU	*Solanum tuberosum*	1797.89	GGETSTNSIASIFAWTR	0.02	0	53	2.3.E-04
					2136.08	EHYLNTEEFIDAVADELK	0.07	0	35	1.1.E-02
					2363.19	EHYLNTEEFIDAVADELKAR	0.04	1	43	1.5.E-03
13	Pyrophosphate-fructose 6-phosphate 1-phosphotransferase subunit beta	ND	PFPB_SOLTU	*Solanum tuberosum*	1660.17	YVVLTPEFIYPYR	0.29	0	29	6.1.E-02
					1845.32	GKYVVLTPEFIYPYR	0.33	1	32	2.6.E-02
74	Pyrophosphate-fructose 6-phosphate 1-phosphotransferase subunit beta	ND	PFPB_SOLTU	*Solanum tuberosum*	1660.03	YVVLTPEFIYPYR	0.15	0	39	5.9.E-03
					1845.13	GKYVVLTPEFIYPYR	0.13	1	28	7.5.E-02
63	Enolase	ND	ENO_SOLLC	*Solanum lycopersicum*	1827.72	IEEELGSEAVYAGASFR	0.15	0	64	2.1.E-05
67	Fructose-bisphosphate aldolase-like protein	gi|2504723	XP_004246552	*Solanum lycopersicum*	2052.28	IGANEPSQLAINENANGLAR	0.23	0	55	9.5.E-03
17	Dihydrolipoamide dehydrogenase precursor	gi|5894612	NP_001275339	*Solanum tuberosum*	2064.36	FLSPSEISVDTVEGGNSVVK	0.31	1	77	7.4.E-05
AMINO ACID/PROTEIN METABOLISM										
6	S-adenosylmethionine synthase	ND	METK_PINBN	*Pinus banksiana*	1775.47	YLDDKTIFHLNPSGR	0.44	1	52	3.4.E-04
7	S-adenosylmethionine synthase	ND	METK_BRARP	*Brassica rapa*	1453.47	FVIGGPHGDAGLTGR	0.28	0	52	3.8.E-04
					1775.55	YLDDKTIFHLNPSGR	0.36	1	61	4.3.E-05
18	S-adenosylmethionine synthase 2	ND	METK2_SOLTU	*Solanum tuberosum*	1526.08	TGTIPDKDILVLIK	0.16	1	36	1.4.E-02
					1776.14	YLDENTIFHLNPSGR	0.26	0	66	1.3.E-05
4	Ferredoxin-nitrite reductase, chloroplastic	ND	NIR_ARATH	*Arabidopsis thaliana*	1278.75	GVVLPDVPEILK	0.01	0	41	5.4.E-03
					1529.86	FGFNLLVGGEESPK	0.04	0	29	6.6.E-02
8	Elongation factor Tu, mitochondrial	ND	EFTM_ARATH	*Arabidopsis thaliana*	1340.94	KFEAEIYVLTK	0.20	1	70	6.5.E-06
					1614.12	TADITGKVELPENVK	0.24	1	40	4.6.E-03
					1649.06	LMDAVDEYIPDPVR	0.28	0	34	2.0.E-02
47	Proteasome subunit beta type-6	ND	PSB6_ARATH	*Arabidopsis thaliana*	1540.73	SGSAADSQVVSDYVR	0.01	0	34	2.2.E-02
					1981.06	YFLHQHTIQLGQPATVK	0.00	0	65	1.3.E-05
DEFENSE RESPONSE										
10	Heat shock cognate 70 kDa protein	ND	HSP7C_PETHY	*Petunia x hybrida*	1436.96	VQQLLQDFFNGK	0.21	0	32	4.1E-02
					1681.08	NAVVTVPAYFNDSQR	0.24	0	52	3.3E-04
					1788.26	IINEPTAAAIAYGLDKK	0.27	1	57	9.5E-05
72	Superoxide dismutase [Fe], chloroplastic	ND	SODF_NICPL	*Nicotiana plumbaginifolia*	1051.64	TFEFHWGK	0.14	0	31	5.2E-02
					1414.89	RPDYISIFMEK	0.19	0	32	4.0E-02
ETC/ATP INVOLVED REACTION										
46	Predicted UMP/CMP kinase-like	gi|261687279	XP_004229700	*Solanum lycopersicum*	1559.76	NQGREDDNIETIR	0.02	1	27	9.7.E-02
					1700.97	KIDAAKPVGEVFEAVK	0.01	1	56	1.2.E-02
57	Vacuolar H^+-ATPase A1 subunit isoform	gi|224682944	XP_006362109	*Solanum tuberosum*	1156.60	LHDDLIAGFR	0.01	0	58	1.3.E-02
9	Adenosine kinase isoform 1S	gi|15186292	AAU14832	*Nicotiana tabacum*	1876.13	ALPYMDFVFGNETEAR	0.27	0	49	4.7.E-02
Others										
12	Cell division control protein 48 homolog A	ND	CD48A_ARATH	*Arabidopsis thaliana*	1569.06	KYQAFAQTLQQSR	0.24	1	61	4.6.E-05

[a] Spot number that corresponds to Prodigy rank number.

[b] Accession number of the top hit sequence from the Solanaceae EST database. ND: Not determined, as a homolog was directly hit from SwissProt.

[c] Accession number of the top hit homolog from MS/MS ion search (MIS) using SwissProt database or MIS followed by EST-based BLAST search using non-redundant protein.

[d] Source organism of the 'homolog' indicated in the left column.

[e] Oxidized Met is underlined.

[f] Number of missed cleavage sites in the tryptic fragment.